UNIVERSIDADE DA BEIRA INTERIOR
Ciências

Desenvolvimento de nanomateriais para aplicação no tratamento de infecções fúngicas

Edgar Silva

Dissertação para obtenção do Grau de Mestre em
Biotecnologia
(2º ciclo de estudos)

Orientador: Prof. Doutor Ilídio Correia
Co-orientador: Mestre Ana Sofia da Silva

Covilhã, Outubro de 2013

When you walk through a storm
Hold your head up high
And don't be afraid of the dark.
At the end of a storm
There's a golden sky
And the sweet silver song of a lark.

Richard Rodgers and Oscar Hammerstein II

Acknowledgments

First of all, I would like to thank my supervisor, Professor Ilídio Correia, for the opportunity he gave me to develop this project. Also, his support and guidance were quite important not only to reach every goal in the work, but also to overtake every difficulty that appeared throughout the year. Moreover, he made this project possible by ensuring all the necessary conditions, from material to reagents, for the development of this work.

I likewise would like to thank my co-supervisor, Ana Sofia Silva, for the teachings, guidance and relevant suggestions that she made at a first stage of the work.

Furthermore, I would like to thank to Eng. Ana Paula from the Optics department of Universidade da Beira Interior for the help in the acquisition of scanning electron microscopy images of the produced nanoparticles, as well as to Susana Ferreira from the microbiology laboratory of Health Sciences Research Centre for all her help and useful advices when working with microorganisms. Thanks to Professor Gilberto U. L. Braga, from the Faculty of Pharmaceutical Sciences of Ribeirão Preto – University of São Paulo, whom I really appreciate for the kindness and availability to send the dermatophytes strains that were crucial to this project completion.

In addition, I would like to thank to all of my group colleagues for all the continuous teaching, support and the good times spent together during the past year.

To my closest friends, housemates and hometown buddies, that have always accompanied me in these last 5 years and were part of this special academic journey. They were always present and helped me to make this master thesis possible. There were great times spent together that encouraged me to move forward, and for this, a big thanks to all of them.

I could not end these acknowledgments without a special thanks to my family, especially my parents and my brother, who were my main support when anything have not worked out the way I would like. I thank them also for all the education, advices and love. Thank you for always believe in me when even myself did not and for the motivation to always move forward. To them I dedicate this dissertation.

Abstract

Dermatophyte infections have been increasing in the last years, and the most common treatments present some disadvantages, like triggering microbial resistance after a continuous application. Therefore, there is a need to develop viable alternatives. Nanotechnology arises as a promising novel multidisciplinary area that is gaining enormous importance in science and technology, having hence, huge potential for biotechnology, biomedical sciences or pharmaceutical industry applications. Silver, which is known since the antiquity by their antimicrobial properties, was used in this work to produce nanoparticles in order to explore its antifungal potential. Nanoparticles have an increased surface area to volume ratio and thus, a contact area that allows a better interaction with microorganisms.

Therefore, herein two different types of silver nanoparticles were produced: silver nanoparticles and silver nanoparticles coated with a polyvinylpyrrolidone (PVP). The nanoparticles produced were characterized by ultraviolet-visible spectroscopy, Fourier transform infrared spectroscopy, scanning electron microscopy, X-ray diffraction analysis and energy-dispersive X-ray spectroscopy. Moreover, the antifungal activity of the two different types of nanoparticles was evaluated and the results showed that they have a good potential for the treatment of infections caused by fungi, since they present similar properties to those of particles previously described in the literature. The toxicity of nanoparticles was also studied, by using keratinocytes from the epidermal layer of the skin, in order to evaluate if the particles kill microorganisms without affecting human cells. The obtained results revealed that the nanoparticles produced have promising properties for their application for therapeutic purposes.

Keywords

Nanotechnology; silver nanoparticles; skin; dermatophytosis.

Resumo

As infecções causadas por dermatófitos têm vindo a aumentar ao longo dos últimos anos e os tratamentos mais usados têm apresentado algumas desvantagens, tais como o desenvolvimento de resistência a estes por parte dos microorganismos. Assim sendo, existe a necessidade de criar alternativas viáveis. A nanotecnologia surgiu recentemente como uma nova área multidisciplinar, que tem permitindo desenvolver novos sistemas com grande potencial em áreas como a biotecnologia, ciências biomédicas e indústria farmacêutica. A prata, conhecida desde a antiguidade pelas suas propriedades antimicrobianas, foi usada no presente projecto para explorar o seu potencial antifúngico na forma de nanopartículas. Estas possuem um maior rácio de área de superfície sobre volume e assim, uma área de contacto que permite uma maior interacção com microorganismos.

Neste estudo foram produzidos dois tipos diferentes de nanopartículas: nanopartículas de prata e nanopartículas de prata revestidas com polivinilpirrolidona. As nanopartículas produzidas foram caracterizadas por espectroscopia UV-visível, espectroscopia de infravermelho por transformada de Fourier, microscopia electrónica de varrimento, difracção de raios-X e espectroscopia de raios-X de dispersão de energia. Além disso, a actividade antifúngica das nanopartículas produzidas foi avaliada usando duas estirpes de dermatófitos e os resultados obtidos demonstraram que as partículas possuem um grande potencial antifúngico, por comparação com os resultados anteriormente obtidos por outros sistemas descritos na literatura. A toxicidade das nanopartículas foi também caracterizada através da utilização de queratinócitos provenientes da camada epidérmica da pele, com o objectivo de determinar se as partículas conseguem eliminar microorganismos, sem afectar as células humanas. Os resultados aqui obtidos revelaram que as nanopartículas de prata produzidas poderão ser usadas na medicina no combate a infecções dérmicas que sejam causadas por fungos.

Palavras-chave

Nanotecnologia; nanopartículas de prata; pele; dermatofitoses.

Resumo alargado

Actualmente, as infecções fúngicas causadas por agentes designados como dermatófitos afectam a pele, couro cabeludo ou até unhas e atingem mais de 20% da população mundial. Os agentes responsáveis podem ser adquiridos nos locais mais comuns, como por exemplo em equipamentos desportivos contaminados, roupa, assim como em balneários e até dormitórios. Apesar de esta não ser uma condição mortal para o ser humano é de um tremendo incómodo, visto poder causar bastante desconforto ao paciente. Após a ocorrência deste tipo de infecções é necessário erradicá-las de uma forma rápida, mantendo o bem-estar do paciente. Existem hoje em dia diferentes fármacos capazes de o fazer, no entanto, estes trazem algumas desvantagens tais como o baixo tempo de residência no local de acção, alguns efeitos secundários e por fim, após uma aplicação prolongada destes, os agentes patogénicos adquirem resistência aos agentes antifúngicos. Esta situação tem despoletado a necessidade de desenvolver novas formas alternativas de combater estas infecções causadas por dermatófitos. A nanotecnologia, que é uma área científica interdisciplinar e que se baseia na aplicação de estruturas a uma escala nano, tem permitindo produzir nanomateriais com características antifúngicas para combater infecções causadas por fungos.

A prata é conhecida por possuir propriedades antimicrobianas, desde o tempo de civilizações como a Egípcia, Grega ou Romana. Este material inorgânico tem assim algumas características muito interessantes como ser um material duradouro, ter alta condutividade térmica, alta resistência à oxidação, estrutura cristalina, baixa citotoxicidade para células humanas, estabilidade a altas temperaturas, baixa volatilidade e por fim um grande rácio entre área de superfície e o volume, o que permite ter um grande número de átomos à superfície e desta forma aumentar a sua interacção com a membrana celular dos microorganismos.

Neste projecto, foram desenvolvidos dois tipos de nanopartículas de prata diferentes: nanopartículas apenas de prata e outras de prata revestidas com polivinilpirrolidona (um polímero solúvel em água). Depois de produzidas as partículas, através de um método de redução química, usando um percursor do metal ($AgNO_3$), e um agente reductor ($NaBH_4$), estas foram caracterizadas por espectroscopia de UV-visível, espectroscopia de infravermelho por transformada de Fourier, microscopia electrónica de varrimento, difracção de raios-X e por espectroscopia de raios-X por dispersão de energia.

A caracterização destes dois tipos de partículas produzidos permitiu concluir que sendo a prata à nanoescala muito reactiva, as partículas contendo apenas este elemento têm uma tendência muito maior para se agregarem e aglomerarem entre elas, perdendo assim a sua estrutura e tamanho originais. Utilizando o polímero para efeitos de revestimento, as partículas conseguem manter-se estáveis e separadas ao longo do tempo, evitando assim a

agregação indesejada das mesmas. Este tipo de fenómeno pode também ser importante para o desempenho das partículas na actividade antimicrobiana a na citotoxicidade que poderão ter para as células humanas. A actividade antifúngica das partículas foi analisada recorrendo à determinação da concentração mínima inibitória por um teste de microdiluições sucessivas e posterior ensaio de resazurina. Duas das estirpes mais comuns de dermatófitos, *Trichophyton rubrum* e *Trichophyton mentagrophytes*, foram usadas neste estudo. Os resultados obtidos revelaram que as nanopartículas de prata possuem um grande potencial antifúngico, comparáveis com outros previamente descritos na literatura. As nanopartículas revestidas exercem um maior efeito em ambos os dermatófitos, sendo que o *T. mentagrophytes* é mais susceptível à prata do que o *T. rubrum*. Relativamente à citotoxicidade dos nanomateriais produzidos, através de um ensaio MTS verificou-se que os queratinócitos se mantinham viáveis após estarem 24 e 48h em contacto com as nanopartículas. Os resultados aqui obtidos demonstram aquilo que é referido por diversas vezes na literatura: o efeito adverso das nanopartículas é menor em células humanas do que para os microorganismos, o que é uma propriedade fulcral a ter em conta para a sua utilização futura na aplicação aqui descrita.

Os dois tipos de nanopartículas de prata aqui estudadas e caracterizadas poderão ter uma futura aplicação no tratamento de infecções causadas por dermatófitos, eliminando assim este trauma que afecta a população em todas as partes do mundo.

Table of Contents

List of Figures

Chapter I – Introduction

Chapter III – Results and Discussion

List of Tables

Chapter I – Introduction

Chapter II – Materials and Methods

Chapter III – Results and Discussion

List of Acronyms

Ag	Silver
$AgNO_3$	Silver nitrate
AgNP	Silver nanoparticles, uncoated
AgNP:PVP	Silver nanoparticles, coated with PVP
AgNPs	Silver nanoparticles (in general)
ANOVA	Analysis of variance
ATCC®	American Type Culture Collection®
BSA	Bovine serum albumin
BSL-2	Biosafety level 2
C=O	Carbonyl group
$C_6H_8O_6$	L-ascorbic acid
$-CH_2$	Methylene group
$-CH_3$	Methyl group
CLSI	Clinical and Laboratory Standards Institute
CO_2	Carbon dioxide
DMEM F-12	Dulbecco's modified Eagle medium F-12
DNA	Deoxyribonucleic acid
EDX	Energy-dispersive X-ray spectroscopy
EtOH	Ethanol
FBS	Fetal bovine serum
fcc	Face-centered cubic
FTIR	Fourier transform infrared spectroscopy
GAGs	Glycosaminoglycans
HIV-1	Human immunodeficiency virus-1
K^-	Negative control
K^+	Positive control
KEC	Keratinocyte epithelial cells

MCL	Maximum contaminant levels
MIC	Minimum inhibitory concentration
MOPS	3-(N-morpholino)propanesulfonic acid
MTS	3-(4,5-dimethylthiazol-2-yl)-5-(3-carboxymethoxyphenyl)-2-(4-sulfophenyl)-2H-tetrazolium
$NaBH_4$	Sodium borohydride
NaCl	Sodium chloride
$NaHCO_3$	Sodium hydrogen carbonate
OEL	Occupational exposure limit
-OH	Hydroxyl group
p	p-value
PBS	Phosphate-buffered saline
PDA	Potato dextrose agar
PMS	Phenazine methosulfate
PVP	Polyvinylpyrrolidone
RPMI 1640	Roswell Park Memorial Institute medium
SC	Stratum corneum
SDA	Saboraud dextrose agar
SDH	Succinate dehydrogenase
SEM	Scanning electron microscopy
SPR	Surface plasmon resonance
UV	Ultraviolet
UV-Vis	Ultraviolet-visible spectroscopy
XRD	X-ray diffraction spectroscopy

Chapter I

INTRODUCTION

1.1. Skin

The human skin is known as the largest organ of the body (Metcalfe and Ferguson, 2007; Sachs and Voorhees, 2011), comprising about 15% of the total body weight (Zaidi and Lanigan, 2010). It not only serves as an essential barrier between the internal and external environment but also provides a potential route for the delivery of therapeutic substances such as drugs and vaccines into skin or the body (Prow *et al.*, 2011; Zhang and Michniak-Kohn, 2012)

Moreover, mammalian skin is also involved in the maintenance of fluid homeostasis, thermoregulation, immunological surveillance, self-healing and sensory detection (Zhang and Michniak-Kohn, 2012) and as a protector of internal organs and tissues from external potentially dangerous factors, such as toxic substances, UV radiation, organisms or pathogens (Prow *et al.*, 2011; Zhang and Michniak-Kohn, 2012) it must have a good integrity, mechanical strength and durability (Yildirimer *et al.*, 2012). Skin is self-renewable, every 2-3 weeks a new layer of skin is developed, replacing the older top layers (Yildirimer *et al.*, 2012). It is also an indicator of well-being, health and beauty of the individual (Sachs and Voorhees, 2011). Trauma, injuries and infections may affect the integrity of this complex organ, which is of crucial importance for the maintenance of their structure and functions.

This tissue has a complex three-layered structure (figure 1), composed from the outermost to the innermost by the epidermis, dermis and a subcutaneous layer called hypodermis (Zaidi and Lanigan, 2010; Yildirimer *et al.*, 2012).

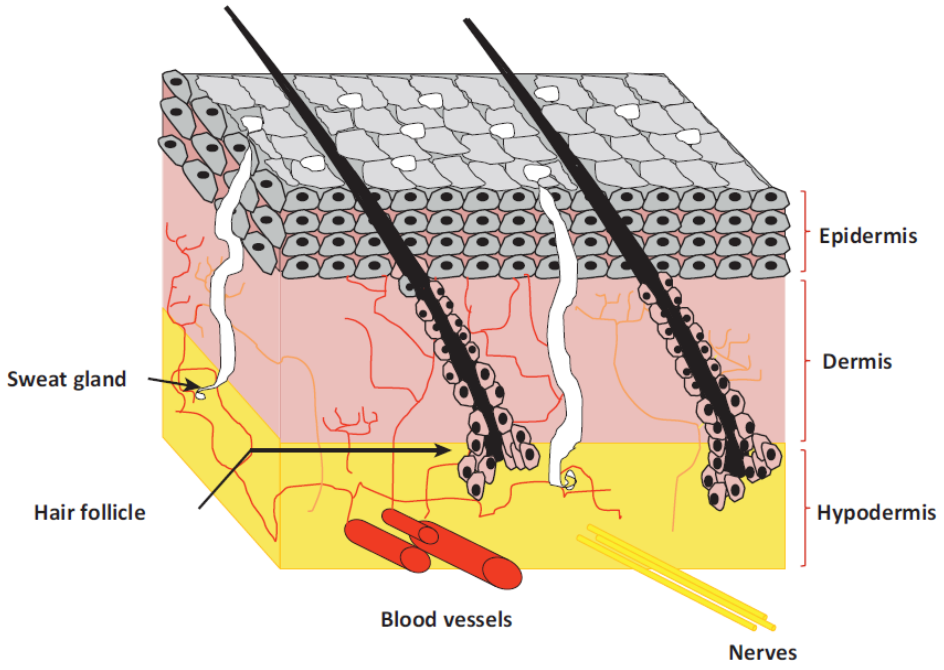

Figure 1 - Illustration of the three-layered human skin including its appendages (adapted from Yildirimer *et al.*, 2012).

1.1.1. Epidermis

The epidermis is a thin layer, barely thicker than paper, which provides a vital barrier function (Metcalfe and Ferguson, 2007; Blanpain and Fuchs, 2009). It has a high cellular content, being composed by about 90 to 95% of keratinocytes (Metcalfe and Ferguson, 2007; Zaidi and Lanigan, 2010). Basal keratinocytes undergo through a process that is known by keratinization. In this process as keratinocytes proliferate, they migrate to the surface of epidermis, becoming differentiated and subsequently forming the various sub-layers (strata) of the epidermis that have distinct functions (Prow *et al.*, 2011; Zhang and Michniak-Kohn, 2012). As an example, the stratum corneum (SC) is the outermost layer of epidermis. The SC represents the main physical barrier of the skin, avoiding water diffusion from this tissue (Prow *et al.*, 2011) and it is based on a lipid-rich "cement", composed by phospholipids, cholesterol and glucosylceramides, localized in the extracellular spaces between dead anucleated corneocytes (Madison, 2003). These dead corneocytes are large and flat differentiated keratinocytes, rich in keratin filaments but without organelles and are held together in a dense pack, which contribute to a more solid layer (Zaidi and Lanigan, 2010). Degradation of the bonds between corneocytes leads to desquamation of the skin (Prow *et al.*, 2011).

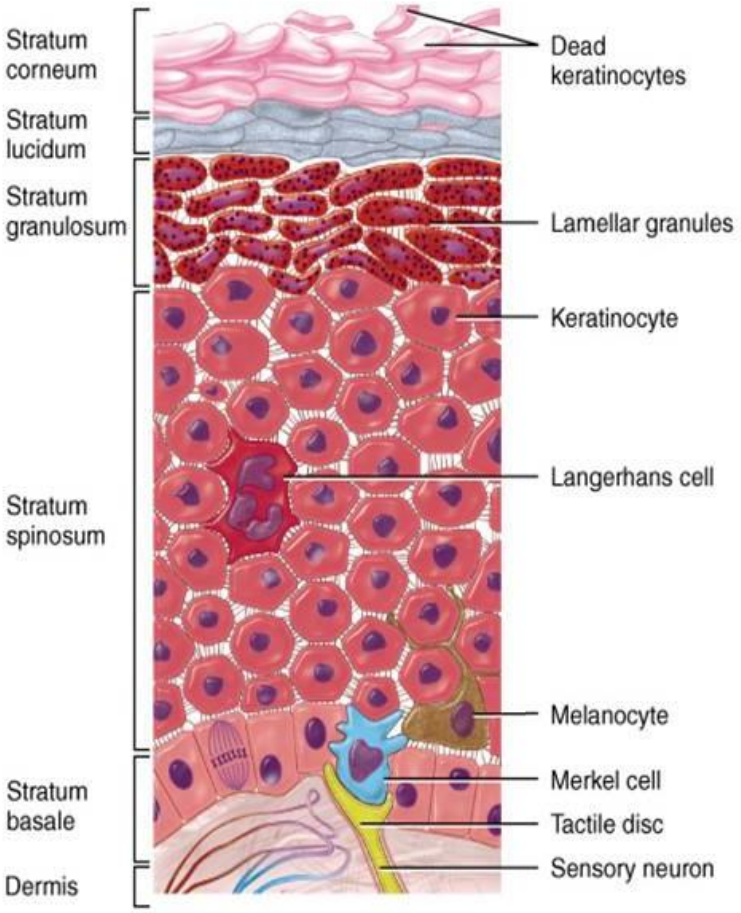

Figure 2 - Structure of the epidermis

(adapted from http://bestofbothworldsaz.com/wp-content/uploads/2010/10/Picture21.jpg on 13-08-13).

Apart from the SC, the epidermis is divided in another 4 strata: the stratum basale; stratum spinosum; stratum granulosum and stratum lucidum (only present in the palms and soles). Table 1 presents some of the structural characteristics from these layers.

Table 1 - Summary of the structural properties of the strata present in the epidermis of skin (Prow *et al.*, 2011; Zhang and Michniak-Kohn, 2012).

Stratum	Characteristics
Corneum	▪ Cornified layer of corneocytes ▪ Possess a "bricks and mortar" structure ▪ Most significant role to the protection barrier in the skin
Lucidum	▪ Thin layer of dead cells ▪ It is only present in the palms and soles, where the skin is thicker
Granulosum	▪ Keratinocytes from lower stratum become granular cells ▪ Cells contain keratohyalin granules ▪ Granules contain proteins that promote hydration and crosslinking of keratin filaments
Spinosum	▪ Layer of spinous cells, where keratinization begins
Basale	▪ Single layer of cells over the basement membrane ▪ Made up basal keratinocyte cells that suffer posterior keratinization and migrate superficially

The skin's outermost layer is not only composed by keratinocytes, which are responsible for the production of keratin that is found in different levels of the epidermis as well as in their own internal skeleton (Zaidi and Lanigan, 2010). However, there are also other cells, presented in figure 2, that have specific functions in the epidermis. Melanocytes are responsible for skin pigmentation, protect it from ultraviolet radiation (through melanin) and are present in the basal layer. Moreover, Langerhans cells, originated from the bone marrow, are present in skin and have tremendous importance in the immunological responses of this organ. Finally, Merkel cells are also present in the basal layer, near the hair follicles and contribute for sensory perception (Zaidi and Lanigan, 2010; Zhang and Michniak-Kohn, 2012).

The epidermis is devoid of any blood vessels and obtains nutrients from the blood vessels that are present in the dermis through a dermoepidermal junction, which is a tissue that connects both major layers and allows nutrients diffusion (Zaidi and Lanigan, 2010). The innermost basement membrane of the epidermis is rich in extracellular matrix proteins and growth factors and due to this, the epidermis adheres to the connective tissue. Moreover, the basement membrane serves not only as a growth-promoting platform but also as a physical boundary between the epidermis and dermis (Blanpain and Fuchs, 2009).

1.1.2. Dermis

The dermis is located right below the epidermis. It is the main component of skin and is described as the tough fibrous layer that has as principal function conferring mechanical support (Metcalfe and Ferguson, 2007; Zaidi and Lanigan, 2010). Dermis consists mainly of collagen, elastin and glycosaminoglycans (GAGs). Fibroblasts are the most abundant cells in this layer, although there are also adipocytes, dermal dendrocytes, histiocytes, macrophages, mastocytes and nerve cells (Zhang and Michniak-Kohn, 2012). Moreover, dermis also contains lymphatic and blood vessels (Metcalfe and Ferguson, 2007; Zaidi and Lanigan, 2010). Briefly, collagen is responsible for skin's appearance (Sachs and Voorhees, 2011) and mechanical support, being its main component (Zaidi and Lanigan, 2010). Elastin is involved in the elastic recoil of the skin and its damage is the main cause of wrinkles (Zaidi and Lanigan, 2010). GAGs, which include heparan sulfate, chondroitin sulfate, dermatan sulfate, and hyaluronic acid are complex polysaccharides that play important roles in cell growth, migration, differentiation and morphogenesis (Sachs and Voorhees, 2011). These components confer support to collagen and elastin, have the capacity to hold water and facilitate the migration through the dermis of components such as nutrients, hormones and fluid molecules (Zaidi and Lanigan, 2010). They also play important roles in several physiological events, such as wound healing and inflammatory response (Clark *et al.*, 2007; Yamada *et al.*, 2011). Fibroblasts are also responsible for the production of other components of the dermis such as collagens, elastins, GAGs and glycoproteins (Zhang and Michniak-Kohn, 2012). Dermal nerve endings are both myelinated and unmyelinated and have a remarkable role in the cutaneous sensations, being involved in preventing injuries due to heat, cold, pressure, among others (Zaidi and Lanigan, 2010). Blood vessels, besides being involved in nutrients supply, are also responsible for the maintenance of body temperature (Zaidi and Lanigan, 2010).

1.1.3. Hypodermis

Hypodermis is described by some authors as the third subcutaneous layer and it is mainly composed by adipose and connective tissue (Yildirimer *et al.*, 2012). The adipose tissue is well vascularized and is involved in the thermoregulation and mechanical support of the whole skin (Metcalfe and Ferguson, 2007).

1.1.4. Appendages

In addition to the structural components of skin, there are also some appendages associated with epidermis and dermis that have different functions (Zhang and Michniak-Kohn, 2012). Hair follicles, sebaceous and sweat glands and nails are examples of these appendages (Blanpain and Fuchs, 2009). Hair follicles have an active role in the wound healing process, since they promote keratinocyte proliferation during reepithelialization. Moreover, sebaceous glands secrete sebum that is useful to moisturize skin and hair while sweat glands may regulate body temperature by secreting sweat onto the surface of the skin and are involved in the excretion of waste products such as urea. Nails, which lie in the epidermis, protect the fingertips (Zhang and Michniak-Kohn, 2012).

1.2. Dermatophytosis

The homeostasis of human skin is usually affected by several microorganisms, such as bacteria, molds, viruses and fungi (Shahverdi *et al.*, 2007). Fungal infections are common in both temperate and tropical climates with a higher prevalence in the 'in development' countries. Dermatophytosis is one example of the infections that can affect skin and was identified in the 19th century. This clinical condition, also known as tinea or ringworm (Moriarty *et al.*, 2012), is a cutaneous fungal infection, or mycosis, caused by three different genera of fungi: *Microsporum*, *Trichophyton* and *Epidermophyton* (Table 2) (Charles, 2009). Such type of fungi are able to invade skin, mucous membranes and other keratinized tissues such as hair and nails (Mayser and Gräser, 2011). They are classified as geophilic, zoophilic and anthropophilic according to their preferred habitat (soil, animals and humans, respectively) (Baldo *et al.*, 2012). The severity of the inflammation is higher in zoophilic infections than in anthropophilic ones (Charles, 2009).

Table 2 - Most common dermatophytes found worldwide
(Charles, 2009).

Ten most commonly found dermatophytes worldwide
Trichophyton mentagrophytes, mentagrophytes variant
Trichophyton mentagrophytes, interdigitale variant
Trichophyton rubrum
Trichophyton tonsurans
Trichophyton verrucosum
Trichophyton violaceum
Microsporum canis
Microsporum canis ferrugineum
Microsporum canis gypseum
Epidermophyton floccosum

Warm and humid conditions are ideal for the growth of fungi that cause the infections described above. They can be spread by the use of contaminated combs, hairbrushes, sports goods, towels and clothing in general. Fungi grow in places such as locker rooms, tanning beds, swimming pools and dormitories. The infection usually affects immunocompromised individuals of any age, with poor hygiene and malnourished (Charles, 2009). Sometimes, the infection may have an acute effect, thus being rapidly eliminated through an efficient and specific immune response. However, some types of dermatophyte species, like *T. rubrum*, the most common anthropophilic dermatophyte (Moriarty *et al.*, 2012), reach a high degree of adaptation in their host and may cause chronic infections with a little or even inexistent symptoms (Vermout *et al.*, 2008). A direct contact is sufficient to transmit the infection from one host to another (Charles, 2009). In skin, the pathogenic agents are found in the SC and exceptionally in the living epidermis. The invasion begins with the penetration of germ tubes (outgrowth) from anthroconidia (fungal spores) into the SC. Once this first step is completed, dermatophytes invade keratinized structures and digest them, using secreted proteases, into short peptides and aminoacids to be assimilated as nutrients (Baldo *et al.*, 2012). Causative fungus may vary according to the different regions of the world, affecting distinct parts of the the body (Charles, 2009) and act in different ways, using distinct proteases. Hence, understanding the pathophysiological mechanisms involved in a dermatophyte infection is the

basis for the development of novel therapeutic strategies (Vermout *et al.*, 2008; Baldo *et al.*, 2012).

Figure 3 - Tinea pedis (athlete's foot) in an infant caused by *T. rubrum* (adapted from Mayser and Gräser, 2011).

Over the past decades, the number of cases of skin mycosis has increased. In fact, more than 20% of the world's population is affected by, at least, one of the dermatophytosis conditions presented in table 3 (Havlickova *et al.*, 2008). Due to this, this infection is one of the most common skin diseases (de Souza *et al.*, 2012). Nevertheless, infections like athlete's foot (figure 3) are not associated with death, although the discomfort and embarrassment that they cause can be quite problematic to the patient (Charles, 2009).

Table 3 - Different types of tinea and respective clinical manifestations and infectious agents (Moriarty *et al.*, 2012).

Different types of tinea		
Tinea	**Clinical manifestations**	**Infectious agents**
Tinea barbae	Beard	*Trichophyton verrucosum* *T. mentagrophytes*
Tinea capitis	Scalp, eyebrows, eyelashes	*T. tonsurans* *T. violaceum* *T. soudanense* *Microsporum canis* *M. audouinii*
Tinea corporis	Trunk	*T. rubrum* *T. tonsurans* *M. canis*
Tinea cruris	Groin, pubic area	*Epidermophyton floccosum* *T. rubrum* *T. interdigitale*
Tinea faciei	Face	*T. verrucosum* *T. mentagrophytes* *T. tonsurans*
Tinea incognito	Erythema that looks indistinct	Any dermatophyte
Tinea manuum	Hand	*T rubrum* *T. mentagrophytes*
Tinea pedis (athlete's foot)	Feet	*T. rubrum* *T. interdigitale* *E. floccosum*
Tinea unguium (onychomycosis)	Nails	*E. floccosum* *T. interdigitale* *T. rubrum* *T. verrucosum*
Tinea versicolor	Trunk, neck	*Malassezia spp.*

The treatment of dermatophyte infections involves oral or topical formulations, such as creams, gels, lotions and shampoos, which can reduce the risk of side effects (Gupta and Cooper, 2008; de Souza *et al.*, 2012). Currently, several different families of antifungal drugs such as azoles, allylamines and griseofulvin are being used for treatment of dermatophytosis (Gupta and Cooper, 2008). Azoles, which can be divided in imidazoles or thiazoles according to the number of nitrogen atoms in the azole ring, are the main antifungal agents used in topical and systemic therapy. Their mechanism of action is quite common, since they selectively block the synthesis of an essential component of the fungal cell membranes, ergosterol. This occurs due to the inhibition of a cytochrome P450-dependent enzyme (lanosterol 14 α-demethylase) that catalyzes the conversion of lanosterol into ergosterol, leading to an increased permeability and rigidity of the fungal cell membrane (de Souza *et al.*, 2012). The most common formulations of azoles used for the treatment of this type of infections are itraconazole, fluconazole and ketoconazole (Gupta and Cooper, 2008). On the other hand, allylamines exhibit a broader spectrum of fungicidal activity against dermatophytes and their mechanism of action is based on the inhibition of the enzyme squalene epoxidase, presented in figure 4. The inhibition of this enzyme interrupts the conversion of squalene to squalene oxide (Kyle and Dahl, 2004), leading to the blocking of the biosynthesis of ergosterol, impairing fungal cellular integrity and resulting once again in fungal cell death (de Souza *et al.*, 2012). Allylamines usually appear in the pharmaceutical form of terbinafine and butenafine (Singal, 2008).

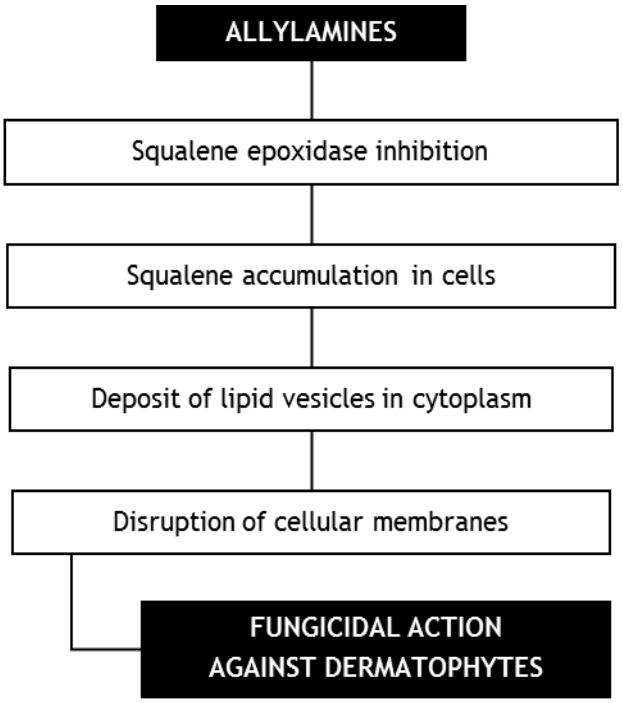

Figure 4 - Example of a mechanism of action of allylamines against dermatophytes (Ryder, 1992).

There are also other types of antifungals like amphotericine B, ciclopirox, amorolfine or even selenium sulfide that contribute to dermatophytosis treatment (Gupta and Cooper, 2008; Monteiro *et al.*, 2011).

Although some of the previously referred antifungals may be highly efficient against these lesions, they have also some disadvantages, such as low residence times at the target site of action, side effects and variable drug permeability, which can also lead to an ineffective dermatophytosis therapy. Furthermore, dermatophytosis treatment is difficult, since it requires long periods of treatment and a lot of determination from the patient (de Souza *et al.*, 2012). Moreover, the lack of rapid and specific diagnosis, drugs toxicity and the development of antifungal resistance, which is recently emerging, demand novel strategies to overcome this type of skin lesions that have become a serious public health problem (Panáček *et al.*, 2009; Monteiro *et al.*, 2011).

1.3. Nanotechnology

To overwhelm the current limitations related to the treatment of dermatophytosis, mostly due to antifungal resistance, it is important to design and develop novel strategies such as new drug delivery systems at a nanoscale level, that may improve the efficacy of existing drugs, or even new products that can have intrinsic antimicrobial properties (Rai *et al.*, 2009; de Souza *et al.*, 2012). Nanotechnology is an interdisciplinary area of science that appeared by the 20th century (Lu *et al.*, 2008) and it is defined by the design, production, characterization, and application of structures, devices and systems at the nanoscale level (Albanese *et al.*, 2012). Typically, nanoscale ranges from 1 to 100 nm (Aruguete *et al.*, 2013), albeit nowadays it is difficult to define an upper limit to that scale (Allhoff and Lin, 2010).

Nanotechnology is gaining a remarkable importance, namely in science and technology with the purpose of manufacturing new materials (Wong and Liu, 2013). It has the capability of modifying metals and polymers, changing radically their chemical, physical, electronic and optical properties. Moreover, reducing a particle size results as well in improving the biocompatibility of certain materials (Kim *et al.*, 2007; Rai *et al.*, 2009). These nanomaterials have features different from that presented by their original-sized equivalents, like greater chemical reactivity, increased surface-to-volume ratio, improved percentage of atoms and useful optical features such as good visible fluorescence (Raffi *et al.*, 2008; Aruguete *et al.*, 2013). These characteristics enable nanoparticles to have mechanisms of action different from the traditional antibiotics and antifungal compounds (Seil and Webster, 2012). Another advantage of nanotechnology relies on the development of rapid and consistent experimental protocols. Such established procedures allow the synthesis of nanomaterials with a wide range of chemical compositions, sizes and dispersity (Singh *et al.*, 2013). Nanotechnology is an emerging area of research that has a variety of applications and

thus, it is expected to be the origin of many of the technological innovations of the 21st century (Singh *et al.*, 2013).

1.4. Silver Nanoparticles

As previously described, nanotechnology is expected to open new insights to fight and prevent several pathologies like cancer and bone/skin related diseases (Morones *et al.*, 2005). Nanosized inorganic particles are fundamental for the development of novel nanodevices that can be used in numerous physical, biological, biomedical and pharmaceutical applications (Kim *et al.*, 2008). Among the most promising inorganic materials are the metallic nanoparticles. Such nanodevices are of great interest not only due to their unique properties but also by their numerous promising applications (Polte *et al.*, 2012). They have a low-cost production processes, increased chemical activity, high efficiency and potential to be applied in the electronic field (Morones *et al.*, 2005; Seoudi *et al.*, 2011). Metallic nanoparticles can be produced with copper, zinc, titanium, magnesium, iron oxide, gold and silver (Rai *et al.*, 2009). Notwithstanding, silver (Ag) has proven to be the most promising material due to its anti-inflammatory properties (Chen *et al.*, 2011), good antimicrobial efficacy against bacteria, viruses and other eukaryotic microorganisms such as fungi, at very low concentrations and without having side effects (Silver, 2003; Gong *et al.*, 2007; Acosta-Torres *et al.*, 2012). Moreover, silver nanoparticles (AgNPs) are cost-saving relatively to gold, and have the ability to readily adjust their optical properties compared to copper (Jiang and Yu, 2010). In fact, silver-based compounds have been extensively used for many bactericidal purposes (Morones *et al.*, 2005). A good example of Ag antimicrobial effect was reported by the Romans, thousands years ago, who treated their water and wine with silver coins (Jain *et al.*, 2009). Ancient civilizations such as Egyptians, Greeks and others, also used silver vessels to store perishable foods and produced silver cutlery, glassware and dishes (Vasilev *et al.*, 2010).

Hippocrates described for the first time the use of silver powder for wound healing and ulcers treatment (Alexander, 2009). Later, in the 17th and 18th centuries, silver nitrate ($AgNO_3$) was effectively used to treat these types of pathologies. Two centuries after, its application was also extended to the treatment of burns and blindness caused by postpartum infections in newborns (Jain *et al.*, 2009; García-Barrasa *et al.*, 2010). However, in 1940, when penicillin was introduced, the use of silver salts to treat bacterial infections decreased. Notwithstanding, its application arose in the later 60s due to the appearance of a 1% silver sulfadazine cream formulation (combination between silver nitrate and sulfonamide) that was used for the treatment of burns (Lee *et al.*, 2008; Rai *et al.*, 2009). This formulation was effective against various bacterial strains, such as *Escherichia coli*, *Staphylococcus aureus*, *Klebsiella spp.* and *Pseudomonas spp.* (Rai *et al.*, 2009). Also, other diseases such as syphilis,

gonorrhea (Alexander, 2009) or even tetanus or rheumatism have historically been treated with silver salts (Vertelov *et al.*, 2008).

Nowadays, due to the emergence of antibiotic-resistant bacteria, clinicians have returned to use wound dressings containing silver (Lee *et al.*, 2008; Rai *et al.*, 2009). However, Ag ions and salts have only a limited efficacy as antimicrobial compounds since Ag is not continuously released from metal. Thereupon, these limitations can be overcome by the use of silver nanoparticles (Kim *et al.*, 2007).

AgNPs are nano-sized structures that are usually smaller than 100 nm and may encompass from 20 to 15,000 silver atoms metallically bonded together (Chen and Schluesener, 2008; Chaloupka *et al.*, 2010). AgNPs are considered a long-lasting material (Monteiro *et al.*, 2009) with great potential to be applied in biomedical and industrial areas (Yen *et al.*, 2009) as an antibacterial, antifungal and also antiviral agent (García-Barrasa *et al.*, 2010; Galdiero *et al.*, 2011). Such nanodevices have attracted a considerable interest due to their unique properties, such as high thermal conductivity, high resistance to oxidation (Song *et al.*, 2009), crystallographic surface structure (Morones *et al.*, 2005), strong shape-dependent optical properties (Zhang *et al.*, 2011), environmentally friendly character (Li *et al.*, 2013), low toxic effects to human cells, high temperature stability, low volatility (Lee *et al.*, 2008; Monteiro *et al.*, 2009) and also large surface-to-volume ratio. This last feature is fundamental for killing microorganisms due to the large fraction of atoms presented in particles' surface, meaning an increased contact area that provides a better interaction with microorganisms (Rai *et al.*, 2009; Bryaskova *et al.*, 2011; Van Dong *et al.*, 2012). In fact, Mansor Bin Ahmad and co-workers referred that AgNPs have a vast bactericidal effect, capable of treating about 650 types of diseases caused by microorganisms (Bin Ahmad *et al.*, 2012). These nanoparticles have revealed bactericidal activity against either gram-positive or gram-negative bacteria species (Panáček *et al.*, 2009), including *Escherichia coli*, *Staphylococcus aureus*, *Bacillus subtilis*, *Streptococcus mutans*, *Staphylococcus epidermidis* (Li *et al.*, 2011) and many others multiresistant strains (Panáček *et al.*, 2009). Moreover, AgNPs have also fungicide activity against strains like *Candida albicans*, *Candida glabrata*, *Candida parapsilosis*, *Candida krusei* and *Trichophyton mentagrophytes* (Li *et al.*, 2011). It was also reported that AgNPs can inactivate viruses, being effective on human immunodeficiency virus-1 (HIV-1), hepatitis B virus, herpes simplex, monkeypox and respiratory syncytial virus (Li *et al.*, 2011). AgNPs show high toxicity to microorganisms while exhibiting low toxicity to mammalian cells (Chen *et al.*, 2011). Moreover, so far no case of acquisition of resistance to AgNPs by pathogenic microorganisms was reported (Monteiro *et al.*, 2011; Acosta-Torres *et al.*, 2012).

Although the bactericidal effect of AgNPs is very well known, their mechanism of action is only partially understood (Morones *et al.*, 2005). Some authors proposed that the ionic silver affects the cell membrane, causing structural changes once AgNPs are attached to it (García-Barrasa *et al.*, 2010). Such modifications include the appearance of pits and gaps leading to the loss of membrane's integrity. Thereby, the essential vesicles that compose the

membrane become dissolved and dispersed. Furthermore, other components such as enzymes that are crucial in the respiratory chain, become disorganized and scattered from their original ordered and close arrangement indicating therefore severe damage and bacteria death (Lok *et al.*, 2006; Li *et al.*, 2011). Other studies refer that ionic silver from the nanoparticles strongly interacts with thiol groups of vital enzymes, for instance succinate dehydrogenase (SDH) and aconitase, inactivating them (Gordon *et al.*, 2010). Moreover, experimental evidences suggest that DNA loses its replication ability, once the bacteria have been treated with silver ions (Morones *et al.*, 2005).

In the case of fungal microorganisms, the mechanism of action of AgNPs is believed to be identical to that proposed for bacteria. This type of nanoparticles affect eukaryotes by attacking their membrane, thus dissipating its electrical potential (Monteiro *et al.*, 2011; Ravishankar Rai and Jumuna Bai, 2011). However, the antifungal effect of AgNPs has received only marginal attention and just a few studies on this topic have been published so far (Xu *et al.*, 2013). Most of these studies have been performed to characterize the effect of Ag in candidiasis infections, in particular the Candida genus, which can be comparable to the genus studied here (Noorbakhsh *et al.*, 2011). Kim and coworkers showed that AgNPs may exert antifungal activity also by inhibiting the normal cell budding process. Leakage of ions and other compounds from the cell, such as glucose and trehalose, occurs as well. These events arise from the perturbation of the membrane lipid bilayers, caused by AgNPs (Kim *et al.*, 2009).

The positive charge of Ag ions is of crucial importance for its enhanced antimicrobial activity due to the electrostatic attraction between the negative charged cell membrane of the microorganism and the positive charged nanoparticle. This type of bond will lead to an accumulation of nanoparticles in the cell membrane, causing an increased permeability of it (Noorbakhsh *et al.*, 2011). The pits described above are caused by metal depletion. This will consequently change the membrane's permeability and therefore progressively release different membrane components, such as lipopolysaccharides, proteins, enzymes, and will finally lead to the dissipation of its electrical potential (Noorbakhsh *et al.*, 2011). The accumulation of nanoparticles could also disrupt the cellular membrane permeability barrier, disturbing the membrane lipid bilayers and thus allowing the entrance of AgNPs into cytoplasm. Such entry causes the damage of chemical structures containing sulfur or phosphorus-based functional groups such as DNA chains, leading afterwards to a cell death (García-Barrasa *et al.*, 2010; Noorbakhsh *et al.*, 2011).

AgNPs also present the advantage of being easily prepared and its production can be scaled up by an economic viable process (Morales-Sánchez *et al.*, 2011). There are different methods that can be used to synthesize AgNPs with a precise shape, size and monodispersity (García-Barrasa *et al.*, 2010; Lee *et al.*, 2010; Van Dong *et al.*, 2012).

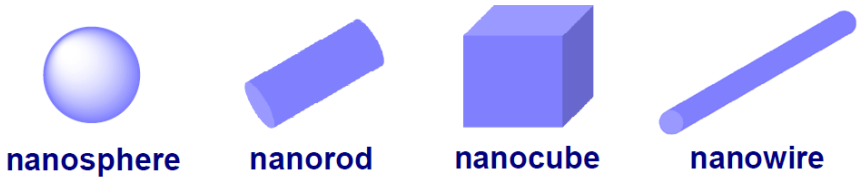

Figure 5 - Different shapes that AgNPs can present (adapted from García-Barrasa *et al.*, 2010).

The new technologies that are being used for AgNPs production include laser ablation (Grade *et al.*, 2012); polyol and radiolytic process (Lee *et al.*, 2010); phase transfer processes, microemulsion, microwave treatment and γ-irradiation (Van Dong *et al.*, 2012); electrochemical, sonochemical, thermal or photochemical processing (Gorup *et al.*, 2011). Nowadays, there is an increased interest in alternative green preparation methods like biosynthetic routes employing either biological microorganisms such as bacteria, fungi, yeast or even plant extracts that contain carbohydrates, alkaloids, steroids and peptides that form complexes with silver ions and produce AgNPs (Hussain *et al.*, 2011). Despite all the aforementioned techniques, the most versatile and used method is still the chemical reduction (Khan *et al.*, 2011). Such procedure presents some advantages over other physical methods, such as high yield and low preparation cost (Lee *et al.*, 2010; Van Dong *et al.*, 2012). The physical methods used for AgNPs production may require high temperatures, vacuum and expensive equipment (Wang *et al.*, 2005). From a chemical point of view, the synthesis of nanoparticles in solution needs methods that allow a precise control over the size and shape of the nanodevices (figure 5), to yield a set of monodisperse colloidal nanoparticles. The production of this type of nanoparticles requires three distinct components: 1) metal precursor, 2) reducing agent and 3) stabilizing agent (García-Barrasa *et al.*, 2010). Particle size and aggregation state of silver are affected by several parameters such as an initial metal precursor concentration, reducing agent/metal precursor molar ratio and also by stabilizer concentrations (Lee *et al.*, 2010). Generally, the most used metal precursor is $AgNO_3$ and then, silver nanoparticles with various shapes can be obtained by using different reducing agents, such as ammonium formate, ascorbic acid, citric acid, dimethylformamide, hydrazine and sodium borohydride (Jiang and Yu, 2010; Hussain *et al.*, 2011). AgNPs characteristics will definitely depend on the strong or weak tendency of substrates to reduce the silver salts (Hussain *et al.*, 2011). The stabilizing agent will not only protect the nanoparticles from the environment but also prevent their agglomeration and precipitation in the colloidal medium (Gorup *et al.*, 2011). It will also play an important role in controlling the size and shape of nanoparticles (García-Barrasa *et al.*, 2010). A few examples of these stabilizing agents are polymeric compounds, such as aminopropyltriethoxysilane, polyacrylates, polyacrylamide, polyacrylonitrile, polyethyleneglycol, polyvinylalcohol and polyvinylpyrrolidone (García-Barrasa *et al.*, 2010). The protection of AgNPs by polymers is gaining importance throughout the years, due to the

higher stability and biocompatibility that they confer to nanoparticles, thus avoiding their aggregation (Monteiro *et al.*, 2009). Furthermore, the capping of AgNPs may result in changes in nanoparticles' physicochemical parameters, such as their charge or agglomeration state, which will affect their biological activity (Grade *et al.*, 2012).

The synthesis of AgNPs can be divided in two stages, nucleation and growth, represented in figure 6. These steps require a high activation energy and low activation energy, respectively. On both stages, reaction parameters such as concentrations, temperature, pH, reducing ability, irradiation, among others, will have influence in the final characteristics of the nanoparticles (García-Barrasa *et al.*, 2010). Hence, chemical reduction of silver ions using different precursors, reducing and stabilizer agents may lead to the production of nanoparticles with different sizes and shapes. Changing just one of these elements or even their concentration is enough to change the morphology of the particles and their general characteristics (Bryaskova *et al.*, 2011).

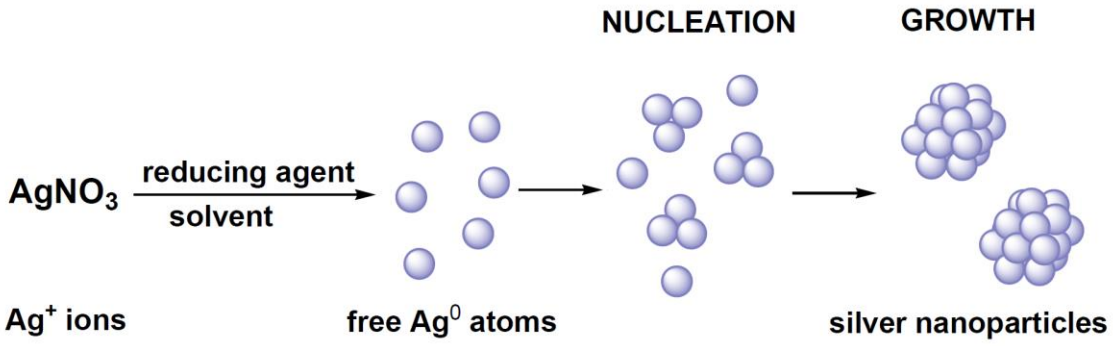

Figure 6 – Representation of the different phases needed for nanoparticles production (adapted from García-Barrasa *et al.*, 2010).

The remarkable antimicrobial activity of AgNPs is a major advantage for the development of products and designing of new applications (Yen *et al.*, 2009). Market segments such as chemical, electronic, food production, optic, packing and textile industries are already using AgNPs in catalytic materials, conductors, detergents, filtration devices, food processing, optical microscopy, sensors and surface-enhanced Raman spectroscopy (Ruparelia *et al.*, 2008; Zielińska *et al.*, 2009; Sadeghi *et al.*, 2010). Furthermore, chopping boards, cookware, dish washers, garbage containers, plastic film, plastic pails, refrigerators and vacuum bottles present, nowadays, nanosilver in their formulations (Zielińska *et al.*, 2009). Due to its significant potential for preventing infections in health fields and wellness services, silver has also been incorporated in products to be used for biosensors, burn dressings, contraceptive devices, cosmetics, dental material, drug carriers, polymers, sunscreen lotion, surgical devices (eg. catheters, implants, prosthesis), textile fabrics and water treatment (Panáček *et al.*, 2009; Yen *et al.*, 2009; Grade *et al.*, 2012) to prevent

bacterial colonization (Lee *et al.*, 2008; Monteiro *et al.*, 2009; Phukon *et al.*, 2011; Bin Ahmad *et al.*, 2012).

Since the application of AgNPs has become more and more widespread in medicine, its presence in the body also increases. Therefore, the consequent toxicological issues in human tissues become quite important and need to be evaluated (Yen *et al.*, 2009). AgNPs have similar sizes to cellular components, or even proteins, so they may bypass the natural barriers and cause harmful effects on living human cells (Yen *et al.*, 2009). Moreover, other potential risks associated with nanocrystalline silver and silver-containing products are the prolonged exposure and ingestion of silver substrates and salts, which may cause conditions such as argyria or argyremia (Silver, 2003; Chen and Schluesener, 2008). Argyria is a rare and irreversible pigmentation of the skin (Kim *et al.*, 2009), while argyremia is related to the elevated silver concentration in blood (Chaloupka *et al.*, 2010). Thereby, in order to avoid the bioaccumulation of silver, maximum contaminant levels (MCL) in drinking water and occupational exposure limit (OEL) have been established (Gong *et al.*, 2007). Nevertheless, compared to other metals, silver exhibits a lower toxicity to mammalian cells (Li *et al.*, 2011). It does not cause any type of allergy (unlike topical antibiotics) (Leaper, 2006) and has not been cited amongst the most prevalent heavy metals in the priority list of hazard substances to public health (Monteiro *et al.*, 2009).

When AgNPs are suspended in liquid (colloidal silver), there are also some limitations associated with the difficulty to control shape, size and stability of AgNPs in colloidal solution (Phukon *et al.*, 2011), since these nanoparticles may undergo oxidation, thus forming aggregates which reduce substantially their antimicrobial activity. In contrast, when double electric layers are formed around AgNPs in colloidal solutions of low ionic strength, agglomeration is inhibited and therefore the particles remain stable along time (García-Barrasa *et al.*, 2010). The combination of smart polymeric architectures, including dendrimers, hydrogels, micelles, microgels, microparticles, multilayered films, nanofibers and vesicles (Agnihotri *et al.*, 2012; Li *et al.*, 2013) with metal nanoparticles, in particular AgNPs, is a promising route to design novel materials with a wide range of applications in biomedical field. In fact, the combination of such polymers and AgNPs has been used to enhance the antimicrobial activity of wound dressings, offering a useful tool to eliminate skin infection and also reduce the risk of appearance of resistant strains (Panáček *et al.*, 2009).

1.5. Objectives

In the present study, the main purpose was to develop materials that have antifungal properties. AgNPs were produced to be used for the treatment of infections caused by dermatophytes. The specific objectives of the workplan herein presented include:

- Synthesis of silver nanoparticles;
- Physico-chemical and biological characterization of the produced nanoparticles at different levels;
- Evaluation of the antifungal activity of the nanoparticles;
- Evaluation of the cytotoxic profile of the nanoparticles.

Chapter II

MATERIALS and METHODS

2.1. Materials

Silver nitrate ($AgNO_3$) and sodium hydrogen carbonate ($NaHCO_3$) were purchased from Panreac (Barcelona, Spain). Polyvinylpyrrolidone (PVP) was acquired from BDH Chemicals Ltd (Poole, United Kingdom).

For cellular culture, keratinocyte epithelial cells (KEC) were obtained from PromoCell. Dulbecco's modified Eagle medium F-12 (DMEM F-12), Roswell Park Memorial Institute medium (RPMI 1640), phosphate-buffered saline (PBS), L-ascorbic acid ($C_6H_8O_6$), bovine serum albumin (BSA), amphotericin B, trypsin, ethanol (EtOH), sodium borohydride ($NaBH_4$) and chloramphenicol were all purchased from Sigma-Aldrich (St. Louis, MO, United States). Moreover, fetal bovine serum (FBS) was acquired from Biochrom AG (Berlin, Germany). 3-(4,5-dimethylthiazol-2-yl)-5-(3-carboxymethoxyphenyl)-2-(4-sulfophenyl)-2H-tetrazolium reagent (MTS) and electron coupling reagent phenazine methosulfate (PMS) were purchased from Promega (Madison, WI, United States).

Dermatophytes strains *Trichophyton rubrum* ATCC® 28188 and *Trichophyton mentagrophytes* ATCC® 9533 were gently given by Professor Gilberto U. L. Braga, from the Faculty of Pharmaceutical Sciences of Ribeirão Preto – University of São Paulo, Brazil. Potato dextrose agar (PDA) was purchased from HiMedia Laboratories (Mumbai, India), Saboraud dextrose agar (SDA) was obtained from Biokar Diagnostics (Beauvais, France) whilst 3-(N-morpholino)propanesulfonic acid (MOPS) was obtained from Thermo Fisher Scientific Inc. (Hudson, NH, United States). Sodium chloride (NaCl) was purchased from VWR BDH Prolabo (Arlington Heights, IL, United States).

T-flasks for cell culture, 90 mm Petri dishes for fungal growth and 96-well plates were all obtained from Orange Scientific (Braine-l'Alleud, Belgium).

2.2. Methods

2.2.1. Nanoparticles Production

2.2.1.1. Preparation of Silver Nanoparticles

AgNPs were produced by adopting a method previously developed by U.T. Khatoon and colleagues (Khatoon *et al.*, 2011). Briefly, the AgNPs production consists on a metal precursor ($AgNO_3$) and a reducing agent ($NaBH_4$). Firstly, 30 mL of a 0.002 M solution of $NaBH_4$, freshly prepared and kept in an iced bath until use, was poured into a beaker under constant agitation. Then, a solution of 0.001 M of $AgNO_3$ was added dropwise to the reducing agent. The reaction was confirmed by the change of color (from colorless to yellow) and afterwards, was kept stirring for more 30 minutes. The nanoparticles produced by this first method consist only of silver and will be named AgNP.

2.2.1.2. Preparation of Silver Nanoparticles coated with PVP

In a second assay, the same AgNPs were produced but now a protecting agent was added to the solution. A water-soluble polymer, PVP, with a molecular weight of 44000 g/mol was used for this purpose. To prepare these nanoparticles, the same 30 mL of a 0.002 M solution of $NaBH_4$ were transferred into a beaker. Then, 5 mL of 0.002 M $AgNO_3$ were added. Moreover, after the entire solution was added, 5 mL of a previously prepared 0.1% solution of PVP were also poured onto reaction. Once the whole polymer solution was present in the reaction, it was kept stirring for 30 minutes. The same change of color, from colorless to yellow occurred, indicating that the reaction took place successfully and the nanoparticles were produced. Finally, this second type of AgNPs were coated with PVP and hereafter they will be named as AgNP:PVP.

2.2.2. Nanoparticles Characterization

2.2.2.1. Ultraviolet-Visible Spectroscopy Analysis

Ultraviolet-visible (UV-Vis) spectroscopy is one of the most popular, easy and rapid characterization techniques that is used to determine particle formation and evaluate final colloid stability (Lee *et al.*, 2010; Desai *et al.*, 2012). All samples were placed in a 10 mm light path quartz cuvette from Hellma Analytics (Müllheim, Germany). UV-Vis spectra were recorded at room temperature using the UV-1700 PharmaSpec from Shimadzu (Kyoto, Japan)

at 300 nm/min scanning rate, with a wavelength range from 300 to 700 nm, and then analyzed with UVProbe 2.10 software. To follow the Beer-Lambert Law, the solutions analyzed needed to be diluted 5 times.

2.2.2.2. Fourier Transform Infrared Spectroscopy Analysis

The different nanoparticles produced were also analyzed by Fourier transform infrared spectroscopy (FTIR). This spectroscopic tool gives information about the molecular structure of chemical compounds, and it is useful for the characterization of biopolymers (Lawrie *et al.*, 2007). Basically, in this technique, a light beam leaves an interferometer, interacts with the sample and strikes a detector. The interferograms measured while scanning are Fourier transformed to yield a spectrum (Smith, 2011). In this work, the spectra were acquired in a Nicoletis 20 spectrophotometer (128 scans, at a range of 4000 to 650 cm^{-1}) from Thermo Scientific (Waltham, MA, United States) equipped with a Smart iTR auxiliary module.

2.2.2.3. Scanning Electron Microscopy Analysis

The morphology of the produced nanoparticles was analyzed by scanning electron microscopy (SEM). First, the produced nanoparticles were centrifuged at 10,000 rpm for 10 minutes. Pellets containing AgNPs were then ressuspended in ultrapure water and washed three times with successive centrifugations with the previous setup. Then, AgNPs were ressuspended in 100 µL of ultrapure water and subsequently sonicated for 2 hours to let the particles disperse. After, a drop (20 µL) was added to a 15 mm cover glass and the whole set was left air-drying overnight. Afterwards, the cover glass was mounted in an aluminium board using a double-sided adhesive tape. Samples were then coated with gold using an Emitech K550 (London, United Kingdom) sputter coater and analyzed using a Hitachi S-2700 (Tokyo, Japan) SEM, operated at an accelerating voltage of 20 kV with different magnifications (Ribeiro *et al.*, 2009; Gaspar *et al.*, 2011a).

2.2.2.4. X-ray Diffraction Spectroscopy Analysis

X-ray diffraction (XRD) analysis was performed to determine several features of the AgNPs, such as their atomic arrangement, crystalline or amorphous phases and orientation.

In order to apply it, firstly, the samples were lyophilized into a powder through a ScanVac CoolSafe freeze-drier from Labogene (Lynge, Denmark) equipped with an external Vacuubrand RZ 2.5 vacuum pump (Wertheim, Germany). Then, the resulting powder was mounted in silica supports using a double sided adhesive tape. The experiments were

performed over the range of 2θ from 5° to 90° with continuous scans at a rate of 1°/min, using a Rigaku Geiger Flex D-max III/c diffractometer from Rigaku Americas Corporation (The Woodlands, TX, United States) with a copper ray tube operated at 30 kV and 20 mA (Gaspar *et al.*, 2011b).

2.2.2.5. Energy-dispersive X-ray Spectroscopy Analysis

Elemental analysis and chemical characterization were performed through an energy-dispersive x-ray spectroscopy (EDX). Each chemical element has a unique atomic structure and therefore a unique set of peaks on its X-ray spectrum will allow its characterization. EDX analysis of AgNPs was carried out in a field emission electron microscope attached to SEM at an accelerated voltage of 20 keV. In this technique there is an interaction between an X-ray beam and the sample, which may excite electrons located at an inner shell of an atom, leading to their movement outwards the shell. Consequently, the place where the excited electron originally was, becomes free and gets occupied by another electron from an outer shell, with higher energy. Thus, the difference in energy between both shells may be released in the form of an X-ray that is measured by an energy-dispersive spectrometer (Goldstein *et al.*, 2003).

2.2.3. Microbiology

2.2.3.1. Dermatophytes Growth

Two strains of dermatophytes were used in this study, *Trichophyton rubrum* (ATCC® 28188) and *Trichophyton mentagrophytes* (ATCC® 9533). These strains have different growth rates. As these two microorganisms are classified as biosafety level 2 (BSL-2), i.e., have moderate potential hazard to personnel and environment, their manipulation was performed in a laminar flow cabinet. Initially, both strains were sent from Brazil by Professor Gilberto U. L. Braga in filter paper strips. This is a beneficial way to transport microorganisms without having to freeze-drying them. To recover the microorganisms, each strip was placed in a falcon tube vial with RPMI 1640 medium with L-glutamine, buffered with MOPS, pH ≈ 7.0. After a few days in liquid medium, at 30ºC, both strains were then cultured into solid agar plates.

Two distinct agar media were used to verify which one allowed a better sporulation from the fungi strains. Sabouraud dextrose agar (SDA) and potato dextrose agar (PDA) were prepared and supplemented with a bacteriostatic antimicrobial agent, chloramphenicol (50 µg/mL).

2.2.3.2. Determination of Nanoparticles Minimum Inhibitory Concentration for Dermatophytes

After both strains colonies grew, *T. rubrum* with white / beige colonies, and *T. mentagrophytes* with flat colonies and mold appearance were obtained after a few days. Then, they were inoculated in RPMI 1640 liquid medium again. This step of the study is in agreement with the standard recommendations for testing common filamentous fungi from the Clinical and Laboratory Standards Institute (CLSI), document M38-A2 (CLSI, 2008). Thus, to isolate fungal microconidia from the colonies in the agar, 1 mL of sterile 0.85% saline solution was used, covering the colonies. Then, the colonies were gently probed with a loop and transferred to a falcon tube vial, allowing the presence of spores on suspension.

To determine the nanoparticles minimum inhibitory concentration (MIC), which is the lowest concentration of an antifungal agent that significantly inhibits growth of the organism, a broth microdilution test was performed in a 96-well plate (CLSI, 2008).

Firstly, AgNP and AgNP:PVP stock solutions were prepared, and then successively diluted with ultra-pure water. Their final concentrations are presented in table 4.

Table 4 - Concentrations of AgNP and AgNP:PVP prepared to perform the broth microdilution assay and MTS assay

Final concentration of AgNP and AgNP:PVP										
Dilution from stock solution	50%	40%	30%	20%	10%	5%	4%	3%	2%	1%
Conc. of Ag (µg/mL)	13.48	10.79	8.09	5.39	2.70	1.35	1.08	0.81	0.54	0.27

The fungal inoculum used in these assays had a final concentration from 1 x 10^3 to 3 x 10^3 CFU/mL (conidia/mL) (Ghannoum *et al.*, 2004). To achieve this number of conidia, they were counted in saline suspension. Thereunto, the resulting suspension was counted with a hemocytometer (Neubauer chamber) and diluted in RPMI 1640 medium. It is important to keep in mind that a 1:2 dilution of both nanoparticles and inocula happened when they are together in the wells. So, the working antifungal solutions and corresponding inocula were two-fold more concentrated than the final concentrations presented here.

Furthermore, to perform the MIC tests, 100 µL of silver nanoparticles in contact with 100 µL of microbial inoculum were used (n=5), to assure a better reproducibility of the results. The samples were incubated for 72h, at 30ºC.

Afterwards, the MIC for each *Trychophyton* was determined through a resazurin test. This colorimetric procedure involves a change in color from blue (indicating no growth) to purple (indicating partial inhibition) or pink (indicating growth). This reaction occurs in living organisms due to the reduction from the first component resazurin (blue) to resorufin (pink), in the presence of enzymes called diaphorases found in the mitochondria (O'Brien *et al.*, 2000). The reaction occurs for about 12 hours in *T. mentagrophytes* and 36 hours in *T. rubrum*. After that, the fluorescence of metabolized resazurin was measured with a spectrofluorimeter (Molecular Devices, Spectramax Gemini XS) at an excitation/emission wavelength of λ = 560/590 nm, respectively.

Control assays without AgNPs in solution were also performed, being the positive (K^+) prepared without any microbial inoculum and the negative (K^-) exclusively with dermatophyte inoculum in RPMI 1640 medium.

2.2.4. Cell Culture

2.2.4.1. Proliferation of Keratinocyte Epithelial Cells

Cell culture experiments were made with the most abundant cells present in the epidermis, keratinocytes. This type of cells requires DMEM-F12 culture medium, supplemented with 10% (v/v) heat-inactivated FBS, and 1% streptomycin and gentamycin antimicrobial agents. Cells were thawed from liquid nitrogen storage, and then seeded into 75 cm^2 T-flasks. KEC remained incubated at 37ºC, in a 5% CO_2 humidified atmosphere until confluence was obtained.

2.2.4.2. Characterization of the Nanoparticles Cytotoxic Profile

After cell attained confluence, they were trypsinized. This method is based on the detachment of confluent cells from the flask, and it was done by using 0.18% trypsin (1:250), for 3 to 5 minutes at 37ºC (Gaspar *et al.*, 2011a). Then, to recover keratinocytes, the cells were centrifuged at 250 g for 5 minutes and the resultant pellet resuspended in DMEM-F12 medium. To obtain the desired final number of cells, a trypan blue assay was done.

The influence of AgNP and AgNP:PVP in cell adhesion and proliferation was determined after 24 and 48h. KEC, at a density of 20,000 cells per well, were seeded in sterile 96-well plate and cultured in DMEM-F12. The same concentrations of nanoparticles previously used in the MIC assay (table 4) were also used in this test. Cells were incubated at 37ºC, in a 5% CO_2 humidified atmosphere. Cell morphology was monitored using an Olympus CX14 inverted light microscope with an Olympus SP-500 UZ digital camera (Tokyo, Japan) attached to it.

In order to evaluate cell viability and proliferation, a MTS non-radioactive assay was performed. Briefly, this method is based on the reduction of MTS into a water-soluble brown compound called formazan (Raje *et al.*, 2013). The reaction is mediated by dehydrogenase enzymes found in metabolically active cells. Moreover, the amount of formazan dye produced is proportional to the quantity of viable cells, allowing to quantify the amount of living cells by a spectrophotometer (Seil and Webster, 2012). Initially, the medium of every well was removed and replaced with 100 µL of a mixture of DMEM-F12, 20% MTS and 1% PMS reagent. Futhermore, the cells were incubated for 4h with a 5% CO_2 humidified atmosphere and absence of light. Absorbance was measured at 492 nm using an Anthos 2020 microplate reader from Biochrom Ltd. (Cambridge, United Kingdom). For control purposes, wells containing cells in the culture medium without nanoparticles were used as K^- and ethanol 70% was added to wells containing cells and were used as a K^+ (Ribeiro *et al.*, 2009).

2.2.5. Statistical Analysis

Statistical analysis of antimicrobial activity and cell viability results were performed using one-way analysis of variance (ANOVA), using the Dunnett's post-hoc test for control comparisons while multiple comparisons were made with the Newman-Keuls post-hoc test. A value of $p < 0.05$ was considered statistically significant (Ribeiro *et al.*, 2009).

Chapter III

RESULTS and DISCUSSION

3.1. Nanoparticles Characterization

3.1.1. Ultraviolet-Visible Spectroscopy Analysis

In a first stage, UV-Vis spectroscopy was used to characterize the produced nanoparticles. The color of the nanoparticles solution started to change from colorless to yellow after the reaction had occured, indicating the formation of AgNPs (Deivaraj *et al.*, 2005), as observed in figure 7, B. Thus, nanoparticles UV-Vis spectra presented a single and sharp extinction band at 400 nm that arises from the localized surface plasmon resonance (SPR), phenomenon attributed to the AgNPs (Lee *et al.*, 2010; Hussain *et al.*, 2011; Khan *et al.*, 2011).

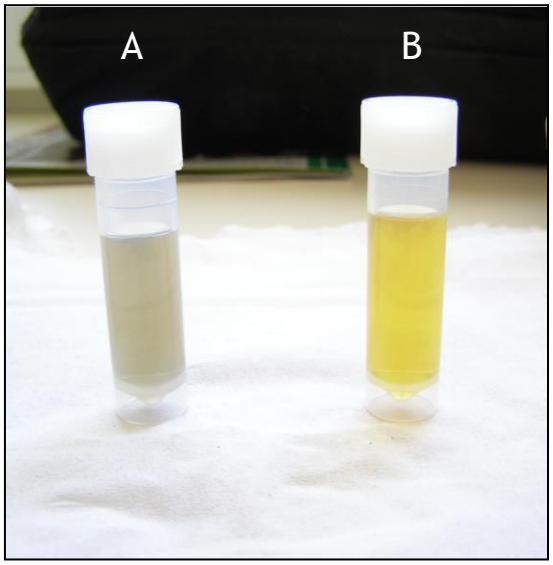

Figure 7 - Colloidal solutions of AgNP (A) and AgNP:PVP (B), 1 month after preparation. The grayish color indicates the aggregation and precipitation of AgNP.

Moreover, AgNPs present a metallic surface, having free electrons in the conduction band and positively charged nuclei (Desai *et al.*, 2012). Then, the SPR of these kind of particles is caused by the multiple excitation of the electrons located near the surface of the nanoparticles. Those electrons are limited to specific vibrations modes according by the particle size and shape (Desai *et al.*, 2012; Jia *et al.*, 2012). For instance, in silver, the conduction and valence bands lie quite close to each other, and that is where the electrons move freely (Desai *et al.*, 2012). Furthermore, the absorption peak is proportional to the quantity of silver present in solution (Bryaskova *et al.*, 2011) and the narrower it is, better dispersed are AgNPs in solution (Lee *et al.*, 2010). UV-Vis absorption spectra are, consequently, very sensitive to the particle size, shape, and aggregation state, since the

AgNPs strongly absorb in the visible region due to the SPR phenomenon referred before (Song *et al.*, 2009).

Through the analysis of figure 8, it can be seen that initially the UV-Vis spectra does not show any sign of sample aggregation, but as the time goes by, the SPR from the AgNP alone changes and the absorption peak becomes broader. 1 day after preparing the AgNP (Fig. 8, spectrum A), they are still with a roughly spherical appearance and the yellow color of the solution is preserved. Moreover, 1 week later (Fig. 8, spectrum B), the spectrum already looks different, being indicative of a variation of AgNP size and shape properties, which may be caused by interactions between particles and aggregation (Song *et al.*, 2009). Also, 1 month after the synthesis (Fig. 8, spectrum C), AgNPs appear to be mostly aggregated, according to its UV-Vis profile.

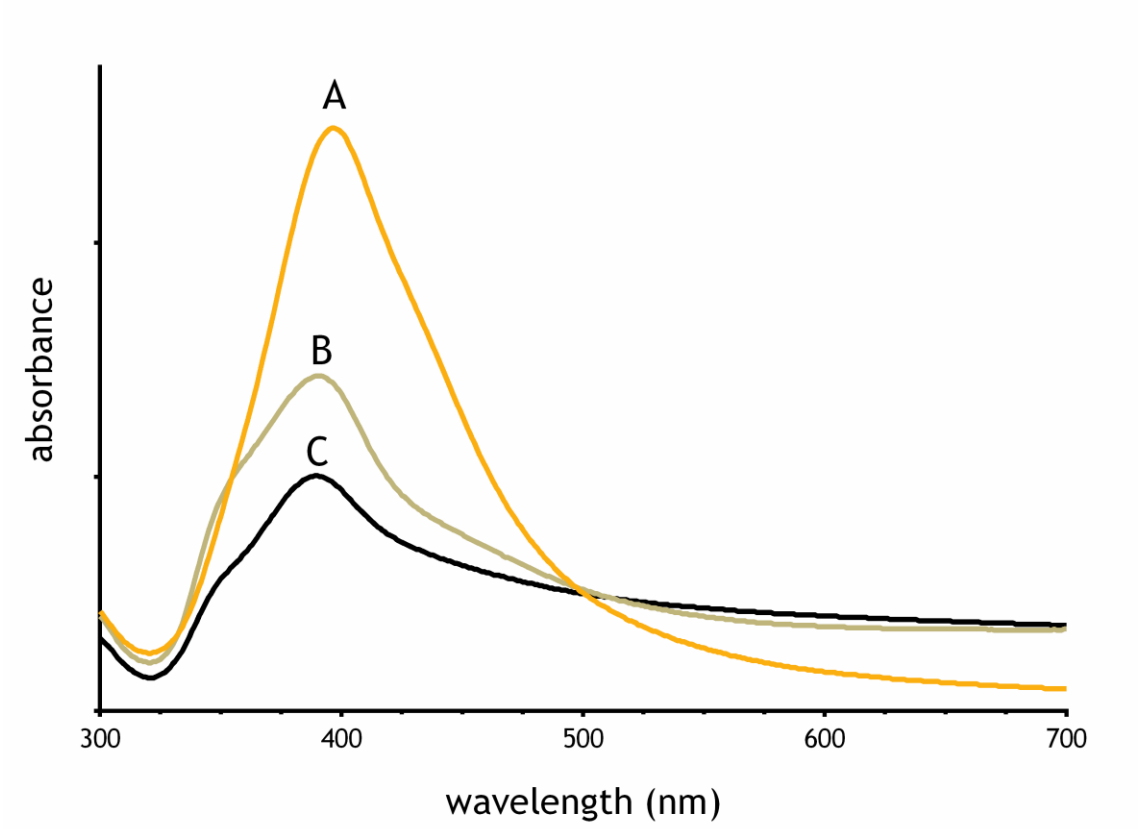

Figure 8 - UV-Vis spectra of AgNP, using solutions with a 1:5 dilution. Profile 1 day (A/yellow), 1 week (B/grey) and 1 month (C/black) after the nanoparticles preparation.

In figure 9, it can be observed that the shape of the plasmon band is symmetrical and quite narrow, suggesting that AgNPs are roughly spherical and monodisperse (Khan *et al.*, 2011; Van Dong *et al.*, 2012). The spectra showed no variation in the shape of the peak at 400 nm after 1 month of storage of AgNP:PVP at room temperature. This means that the solution is quite stable due to the coating performed with PVP and does not show any evidences of particles aggregation (Rathod *et al.*, 2011; Krishnaraj *et al.*, 2012).

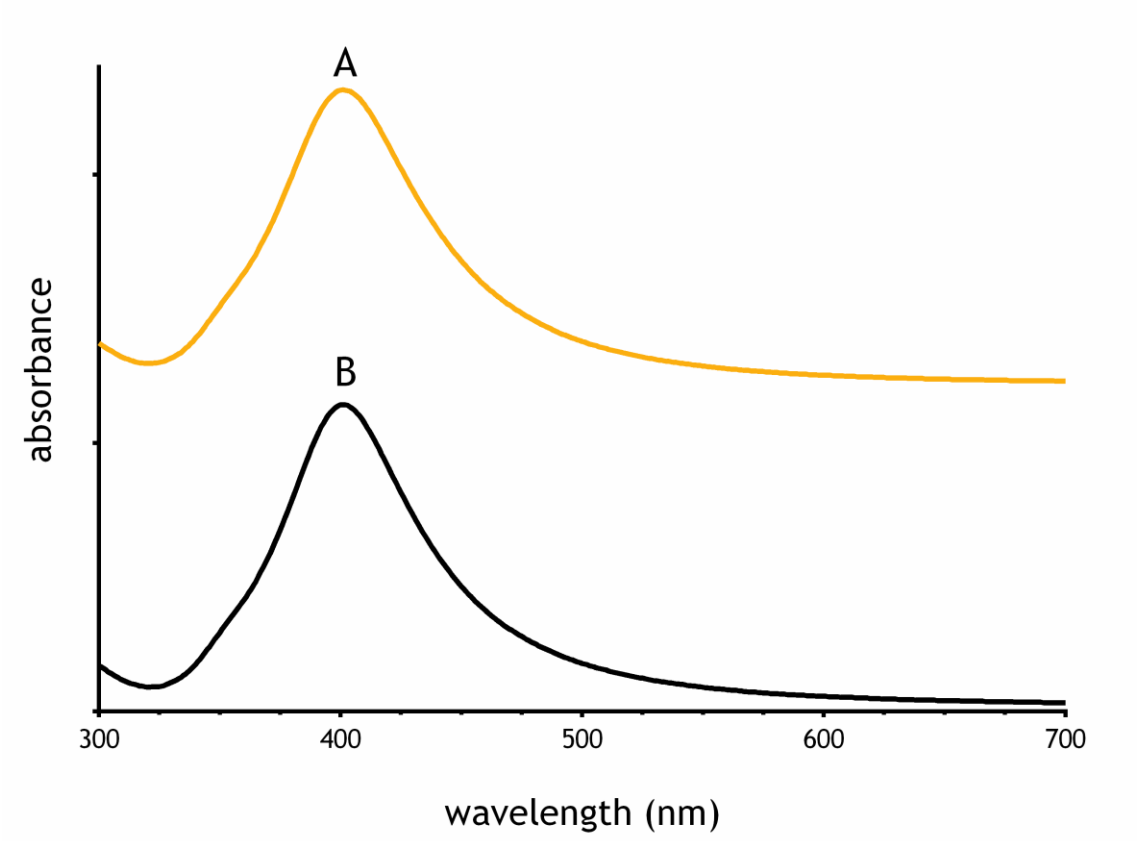

Figure 9 – UV-Vis spectra of AgNP:PVP, using solutions with a 1:5 dilution. Profile 1 day (A/yellow) and 1 month after their production (B/black).

Concluding, the particles present different spectra along time making the evaluation of metallic nanoparticles by UV-Vis spectroscopy through time a reliable method.

3.1.2. Fourier Transform Infrared Spectroscopy Analysis

In order to evaluate the interactions between the AgNPs produced with the silver itself and the protecting agent PVP, FTIR analysis was performed.

By the observation of figure 10, a peak between 3500 cm^{-1} and 3300 cm^{-1} shows the presence of a hydroxyl group (-OH). This means that there is still remaining water in the samples (Zhao *et al.*, 2010). Moreover, through the analysis of the stock solution of PVP (Fig. 10, spectrum B), the smooth peaks represented at about 2951 cm^{-1} and 2922 cm^{-1} are related to the $-CH_3$ and $-CH_2$ symmetric stretching vibration, respectively (Sobczak-Kupiec *et al.*, 2012). Besides these stretching absorptions, in FTIR analysis it can also be seen the deformation absorption from $-CH_3$ and the scissor vibration from $-CH_2$. About $-CH_3$ deformation absorption, two splitted peaks can be seen about 1287 cm^{-1} and 1274 cm^{-1}. Both peaks are a bit displaced from where they were predicted to be (about 1380-1370 cm^{-1}).

Relatively to the -CH_2 scissor vibration, the corresponding band is present nearly 1422 cm^{-1} (Sobczak-Kupiec *et al.*, 2012). These aliphatic hydrocarbons are characteristic of PVP, being an evidence of the presence of the polymer in the nanoparticles. It is also known that PVP contains a tertiary amide, having then a C=O stretching. This stretching can be also verified through FTIR analysis. It consists on the sharp band present at 1644 cm^{-1} (Shin *et al.*, 2004; Singh and Raykar, 2008). All the peaks referred above are characteristic of PVP and their presence was confirmed.

Relatively to the analysis of an $AgNO_3$ solid sample (Fig. 10, spectrum A), a single peak is noteworthy. It is located at 1266 cm^{-1} and allowed to demonstrate that AgNP and AgNP:PVP samples used in this study do, in fact, possess silver in its composition.

Therefore, comparing spectra A and B with the peaks resulting from the nanoparticles samples spectra (Fig. 10, spectra C and D), it can be concluded that either AgNP alone and AgNP:PVP have, as expected, silver in its constitution. The band presented in B is also verified in the same wavenumbers for C and D. In the case of AgNP:PVP, every properties previously described for the polymer were also observed in AgNP:PVP. Furthermore, the peak presented at 1321 cm^{-1} is increased due to the presence of silver, as previously described.

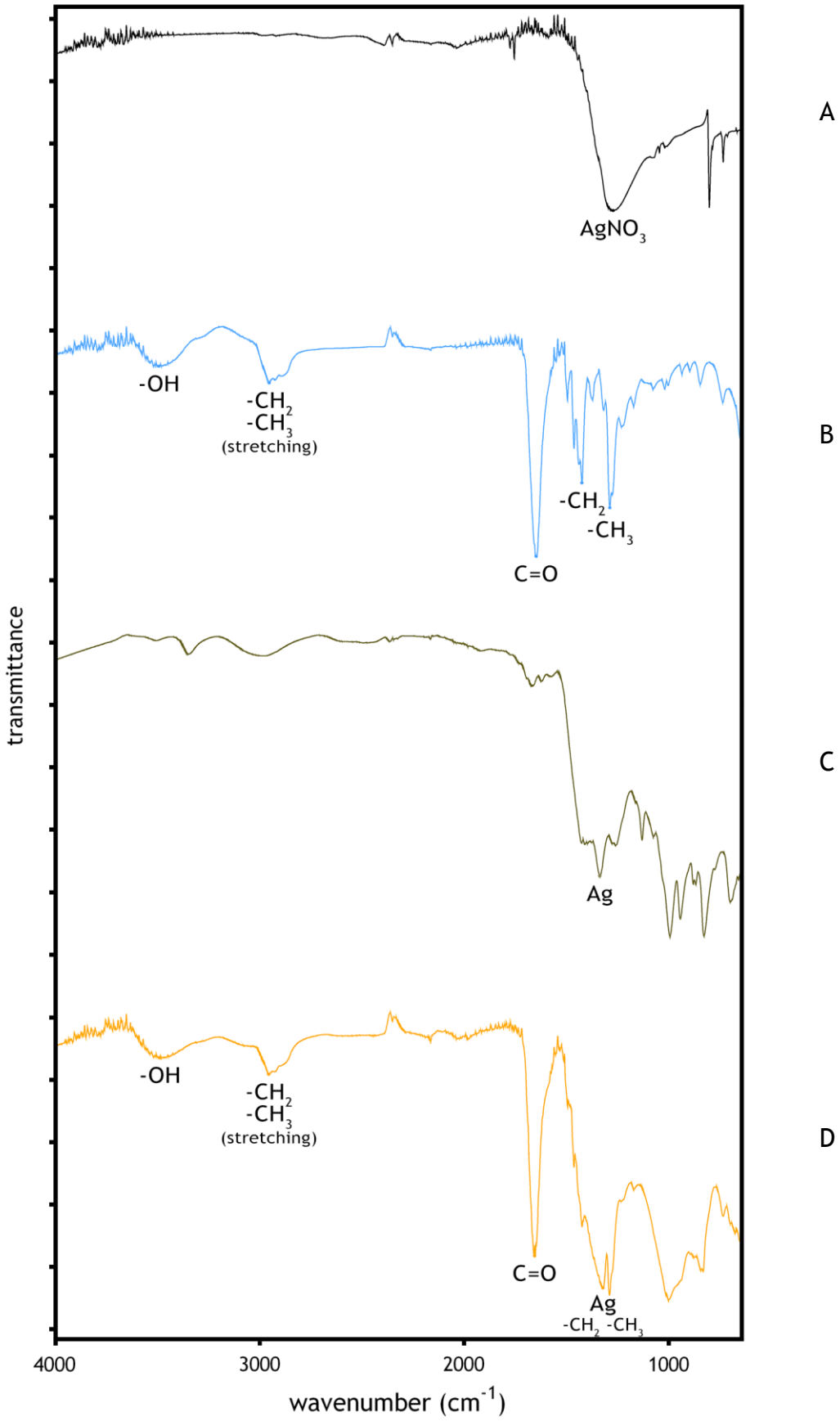

Figure 10 - FTIR spectra of $AgNO_3$ (A/black), PVP (B/blue), AgNP (C/grey) and AgNP:PVP (D/yellow) samples, with their respective characteristic peaks identified.

3.1.3. Scanning Electron Microscopy Analysis

SEM was used to characterize nanoparticles morphology and size. However, due to the small size of the particles, transmission electron microscopy (TEM) would be better in order to perform a deeper characterization of the nanoparticles.

The first difference observed between AgNP and AgNP:PVP is that for AgNP alone more aggregates were seen, while the nanoparticles capped with PVP were quite dispersed and may be easily distinguished in figure 11. The high surface area to volume ratio, characteristic of AgNPs in general, may lead to self-attractions and consequently to particle aggregation with loss of structure. The uncoated AgNP surface charges from silver ions are "naked", which will make this process of agglomeration easier. Therefore, this property may compromise further testing since it may change the antimicrobial potential of these nanoparticles as well as the actual cytotoxic profile of the material (El Badawy *et al.*, 2010).

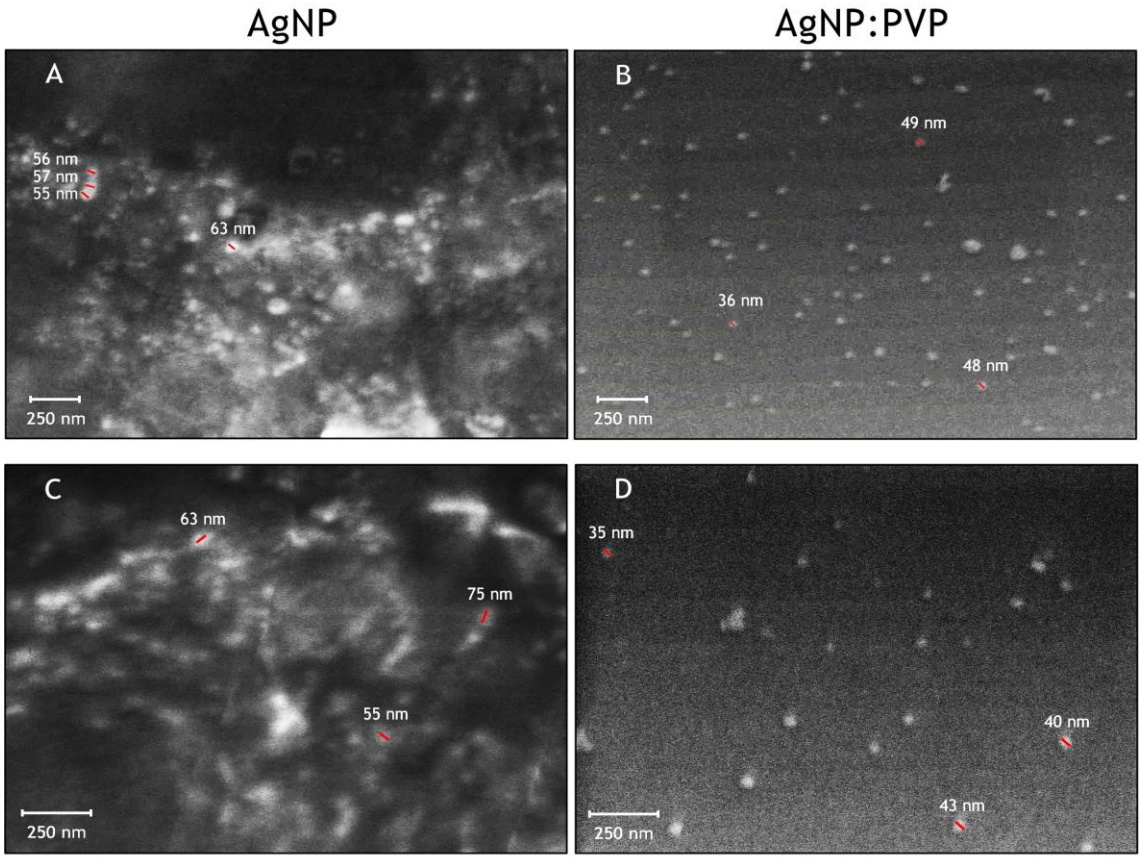

Figure 11 – SEM images of AgNP (A, C) and AgNP:PVP (B,D).

SEM analysis revealed that nanoparticles have a roughly spherical shape. The size of the samples was evaluated by using ImageJ software, developed by National Institutes of Health (Bethesda, MD, United States). Figure 12 presents a histogram based on software measurements, in which AgNP:PVP mostly presented a size between 20 and 60 nm. The average size was approximately 40 nm, which is comparable with other data reported in the literature (Zielińska *et al.*, 2009).

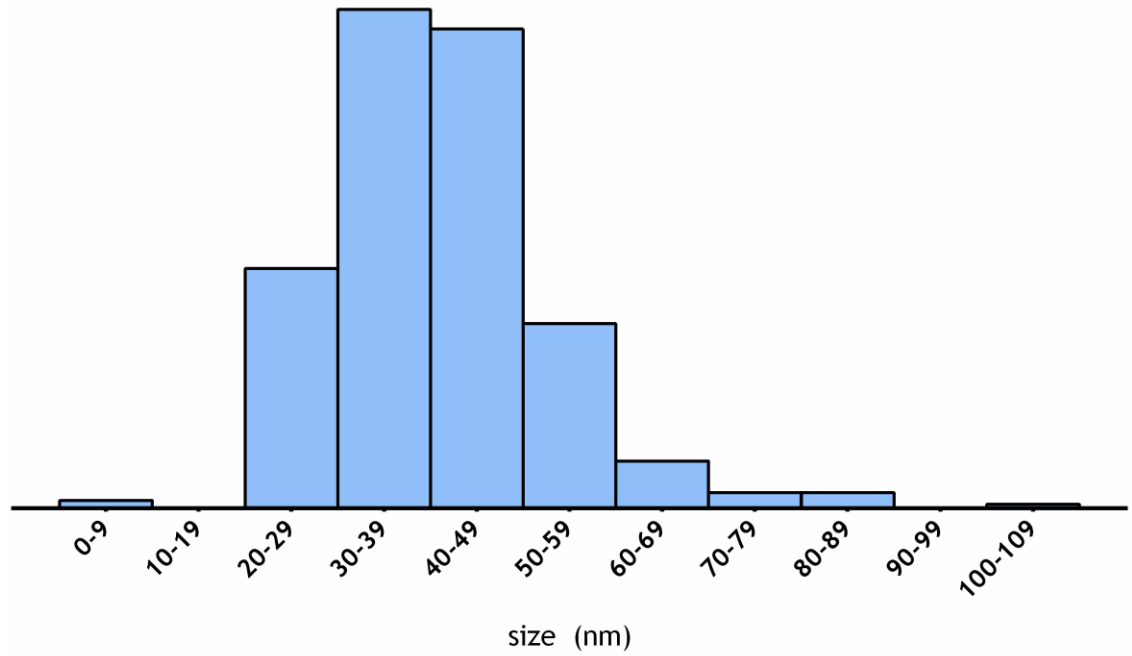

Figure 12 - Histogram based on software measurements of AgNP:PVP, showing an average size of 40.64 nm

3.1.4. X-ray Diffraction Spectroscopy Analysis

The X-ray diffraction analysis is another way to confirm the presence of AgNPs, using a sample in the form of powder (Maneerung *et al.*, 2008). Moreover, this technique allows to determine the physical form of freeze-thawed samples (amorphous or crystalline) and is used to characterize a crystallographic structure, preferred orientation and crystallite size (Khatoon *et al.*, 2011; Gaspar *et al.*, 2011b).

By analyzing AgNP:PVP XRD plot in figure 13, spectrum B, a major characteristic peak can be identified at a 2θ value of 38.2°. This corresponds to the reflections of the crystalline nanoparticles in the face-centered cubic (fcc) structure with basal (111) lattice planes (Van Dong *et al.*, 2012). Other diffraction peaks that are characteristic of Ag are at scattering angles of 44.3°, 64.5° and 77.5°. These reflections correspond respectively to the (200), (220) and (311) sets of crystallographic planes in the fcc structures of silver as well (Monteiro *et al.*, 2011; Seoudi *et al.*, 2011; Nguyen *et al.*, 2012; Singh *et al.*, 2013). Being these last set of planes very weak, it indicates that the AgNP produced with PVP are very anisotropic and

therefore (111) oriented (Singh *et al.*, 2012). Additionally, there are also a few tiny peaks that appear at 20.3°, 29.5°, 30.6° which can be explained by the presence of some compounds that were used for nanoparticles synthesis, such as PVP (Singh *et al.*, 2013).

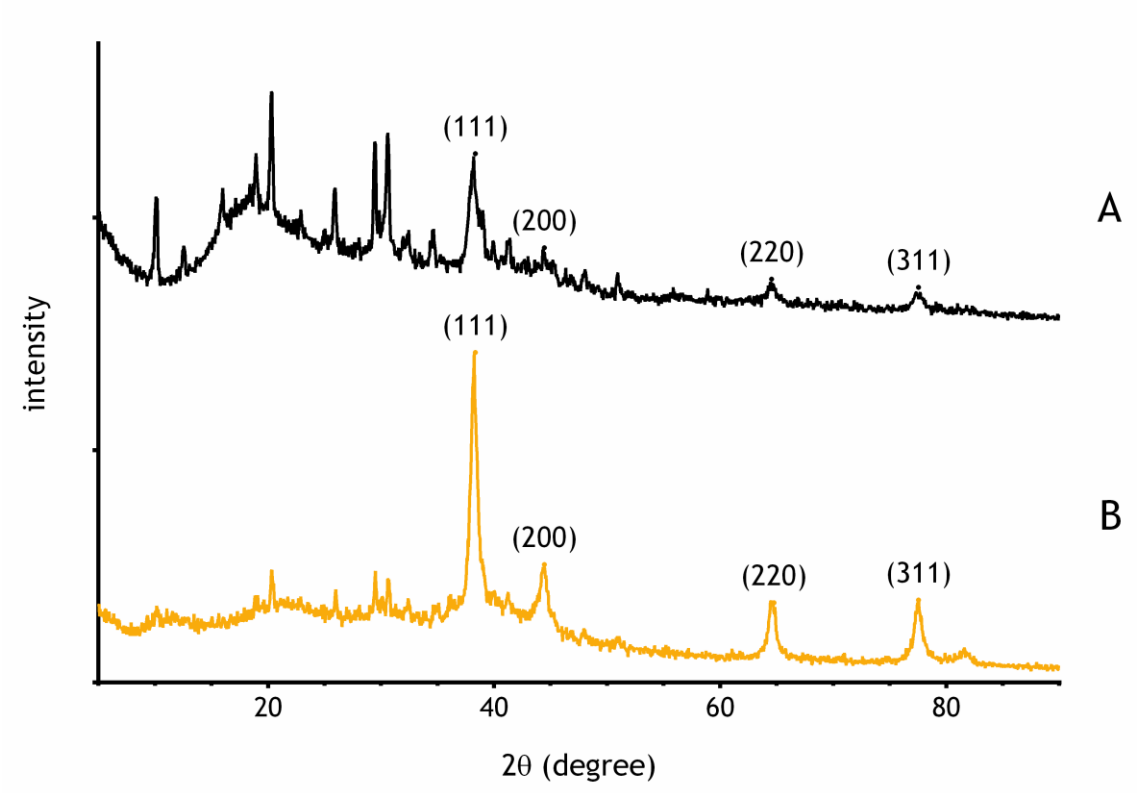

Figure 13 - XRD spectra of a AgNP (A/black) and AgNP:PVP (B/yellow) samples, with the respective peaks corresponding to the different (111), (200), (220) and (311) lattice planes.

Relatively to the analysis of AgNP alone in the same figure (spectrum A), the identical (111) lattice plane can be observed. However, the peak at a 2θ value of 38.2° is not so expressive as in AgNP:PVP. Furthermore, the other three planes previously observed are present but do not have the same regularity. In the AgNP case, there are a lot of additional and unassigned peaks outside the silver standards. This can be explained by the aggregation of the uncapped particles had suffer, which is even superior when the AgNP are subjected to freeze-thaw conditions. The agglomeration leads to the loss of structure from AgNP that is reflected in the XRD spectra.

3.1.5. Energy-dispersive X-ray Spectroscopy Analysis

To identify the elemental composition of the previously prepared nanoparticles an EDX analysis was also performed. Therefore, it is a reliable method to verify if AgNPs contain, in fact, silver at the nanoscale level (Gajbhiye *et al.*, 2009; Khatoon *et al.*, 2011). The EDX profiles of both AgNP and AgNP:PVP samples actually show silver signals between 2 and 4 keV, as expected due to surface plasmon resonance. These peaks are directly related to the silver characteristic lines K and L (Singh and Raykar, 2008; Jiang and Yu, 2010; Vijayakumar *et al.*, 2013). Besides silver, the EDX also showed the presence of carbon, oxygen and copper, by the peaks located at 0.28, 0.52 and 0.93 keV, respectively. Both carbon and copper may be justified by the copper grid and carbon-covered film present on the surface of the SEM grid (Naik *et al.*, 2002; Van Dong *et al.*, 2012). Furthermore, an oxygen peak is also observed, suggesting the presence of an oxide layer in the nanoparticles (Ruparelia *et al.*, 2008).

Moreover, the AgNP:PVP (figure 14) shows a more intense carbon peak in this sample, which confirms the presence of the stabilizer, composed by alkyl chains (Puchalski *et al.*, 2007; Singh and Raykar, 2008).

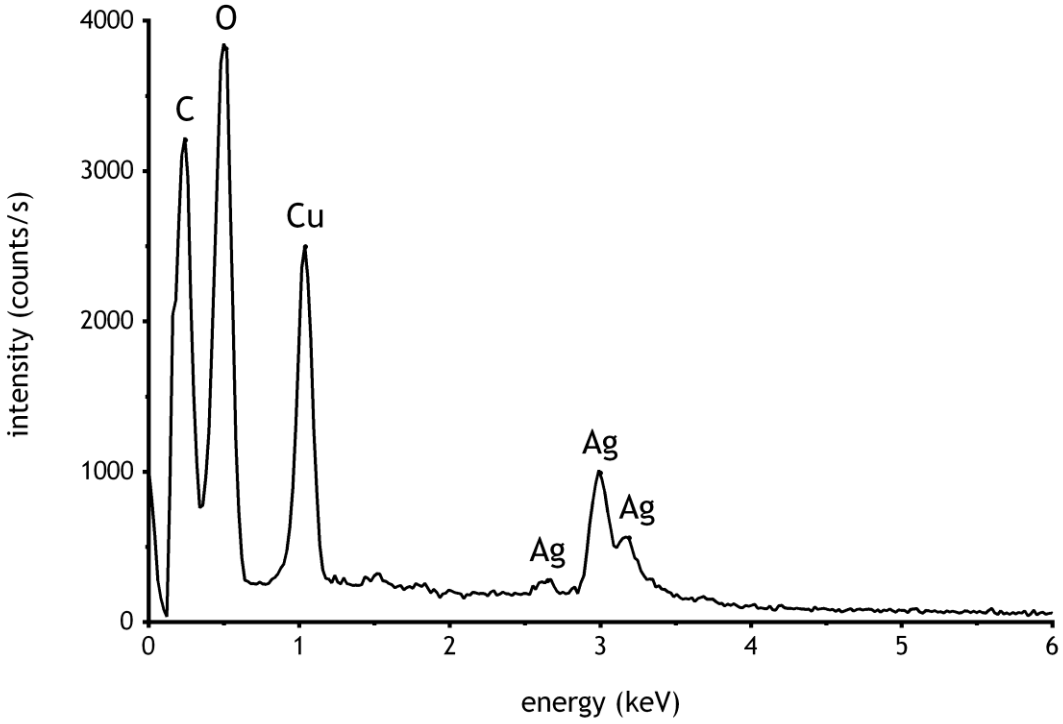

Figure 14 - Elemental analysis of AgNP:PVP.

Still, the oxygen peak is more intense for AgNP samples (figure 15), which can be explained by their lower stability and greater propensity to agglomerate, leading then to an easier oxidation of the nanoparticles.

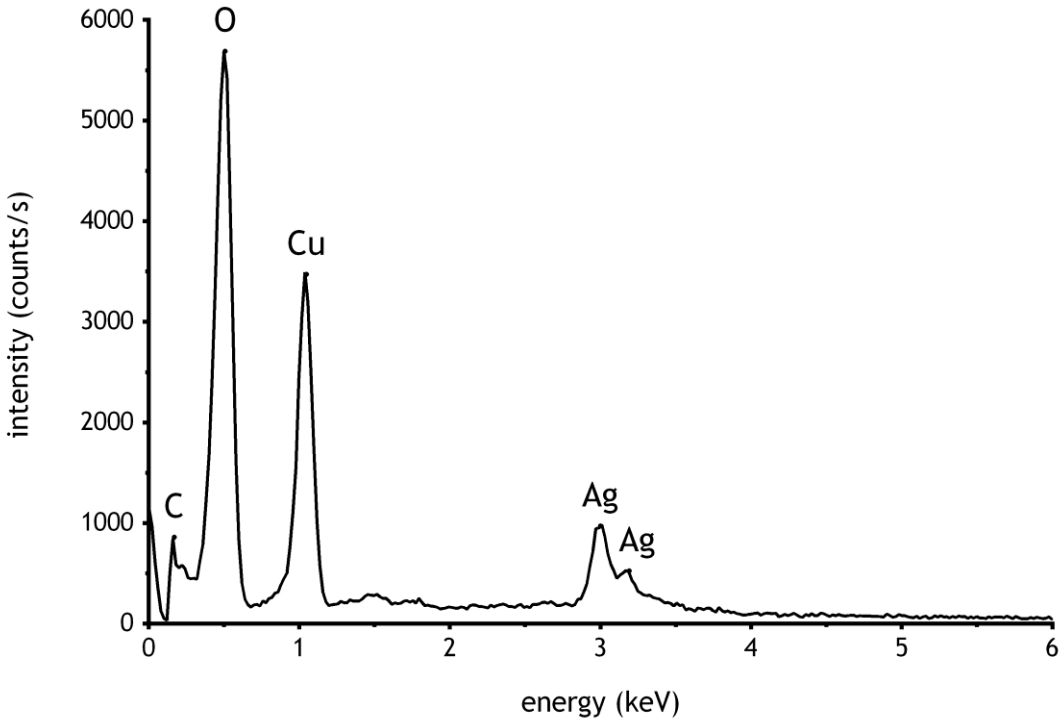

Figure 15 - Elemental analysis of AgNP.

3.2. Evaluation of the Nanoparticles Antifungal Activity

The antifungal properties of the prepared nanoparticles were evaluated against two different dermatophytes: *Trichophyton rubrum* and *Trichophyton mentagrophytes*. The choice of these two strains was based on the fact that these are the most frequently isolated dermatophytes (da Silva Barros *et al.*, 2007).

To evaluate the antimicrobial effects achieved by AgNP and AgNP:PVP, a MIC assay was performed, which is based on a broth microdilution susceptibility test. Furthermore, this assay is an approved standard testing by the Clinical and Laboratory Standards Institute (CLSI, 2008).

Initially, fungal growth was tested by using two different agar media, SDA and PDA. After, *T. rubrum* and *T. mentagrophytes* were left to grow at 30ºC inside an incubator. The macroscopic appearance of colonies in both media was evaluated. At the second day of incubation, little white and well dispersed colonies of *T. mentagrophytes* appeared in both SDA and PDA. Conversely, just in the fifth day *T. rubrum* began to grow, but with more colonies in PDA than in SDA. As for *T. mentagrophytes*, in the fifth day their growth was already quite abundant, presenting in SDA a brownish color while in PDA the colonies were milky colored. In both media, this last culture began to develop mold and they were ready to be used for the MIC assay. The *T. rubrum* strain, at their seventh day of growth in SDA and PDA, the colonies presented a white color, less sporulation than *T. mentagrophytes* and were also ready to be assessed.

After counting microconidia for each strain cultured on the different agar media with the help of a haemocytometer, it was concluded that PDA presented the most sporulated colonies, although limited in *T. rubrum* (Jessup *et al.*, 2000). Colonies cultured in PDA were thus used for further testing.

As previously mentioned, to determine MIC values, both AgNP and AgNP:PVP were diluted with water as indicated by the M38-A2 reference method (CLSI, 2008). The microorganisms were also diluted to a final concentration of 1×10^3 to 3×10^3 CFU/mL as recommended by Ghannoum and colleagues (Ghannoum *et al.*, 2004). MIC was determined after 72h of incubation at 30ºC and was evaluated throughout a resazurin assay. This assay is based on a non-toxic measurement of the metabolic activity of living dermatophytes by determining the concentration of resorufin. Resofurin is a pink fluorescent compound produced by reduction of resazurin (7-hydroxy-3H-phenoxazin-3-one-10-oxide) by viable living microorganisms (O'Brien *et al.*, 2000). To verify the reproducibility of the results, all antimicrobial activity assays were performed in quintuplicate.

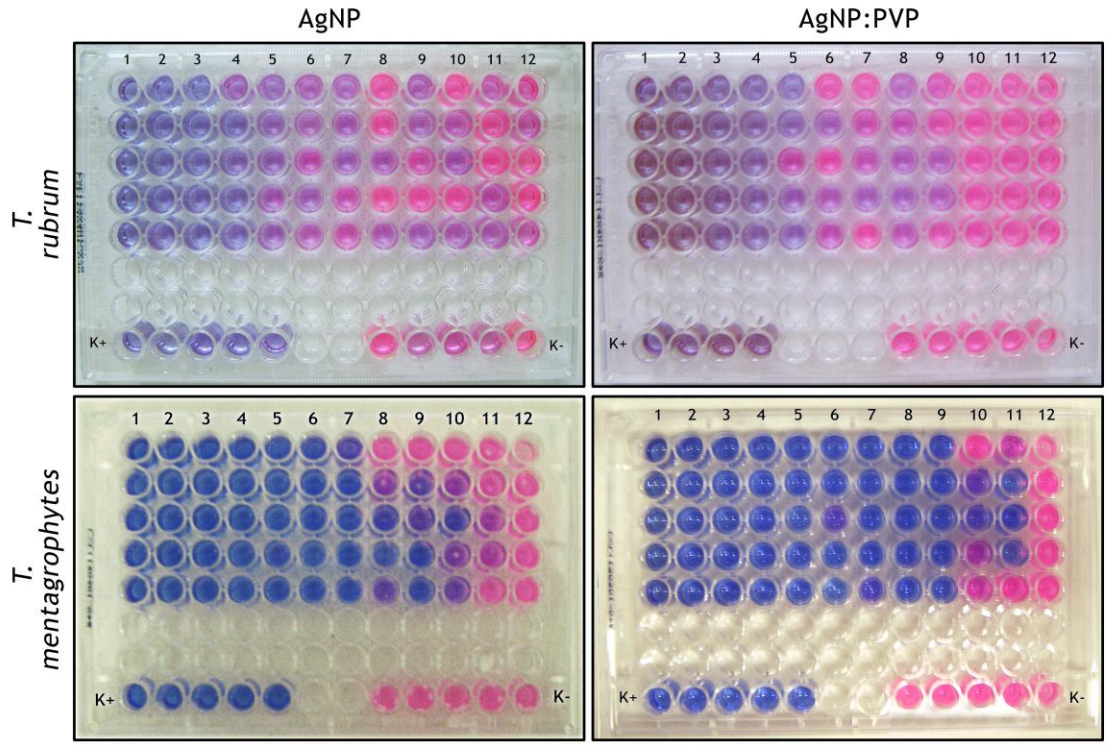

Figure 16 – Images of 96-well plates showing a resazurin assay to evaluate the antifungal activity of AgNP (first column) and AgNP:PVP (second column). Two different dermatophyte strains (*T. rubrum* and *T. mentagrophytes*) were used. Nanoparticles concentrations (µg/mL): 1) 13.48; 2)10.79; 3) 8.09; 4) 5.39; 5) 2.70; 6) 1.35; 7) 1.08; 8) 0.81; 9) 0.54; 10) 0.27; 11) 0.135; 12) 0.0067. The positive control without any microorganisms is represented by K^+ and the negative control composed only by the fungal inocula is represented by K^-.

In figure 16, wells presenting a bluish color reveal effective fungal growth inhibition. The pink color represents the converted resofurin presented in the well, meaning that the microorganisms are present and the desired dermatophytes death did not occur. Despite this colorimetric results, which are visible macroscopically but present discrepancies that hamper the determination of a certain inhibitory concentration, the fluorescence of metabolized resazurin was also determined by using a spectrofluorimeter.

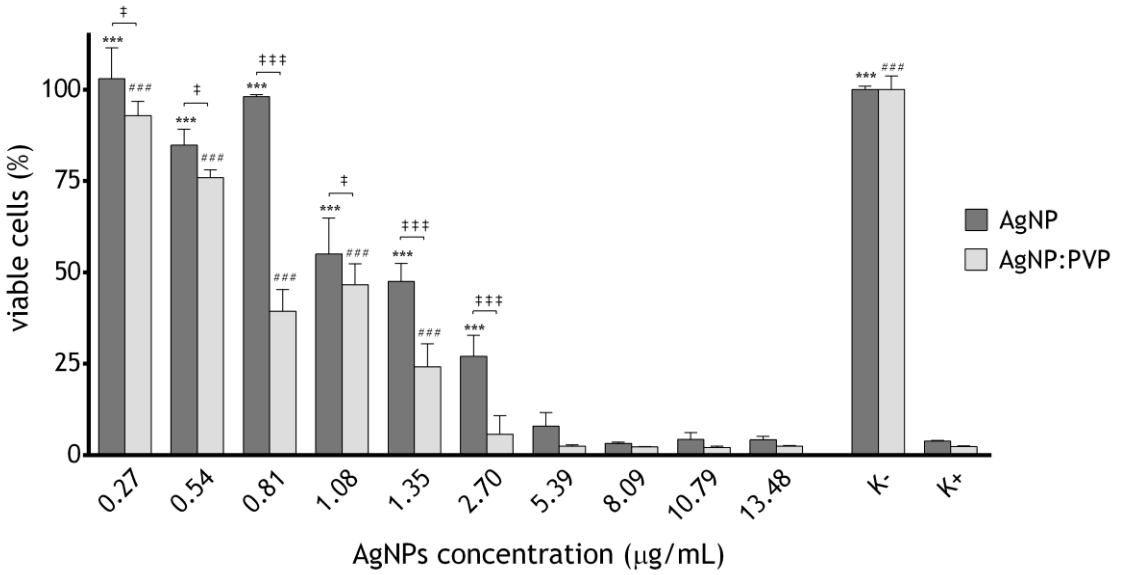

Figure 17 – Antifungal activity of two different types of nanoparticles produced for *T. rubrum*. Negative control (K^-), positive control (K^+). Each result is mean ± standard error of the mean of at least three independent experiments. Statistical analysis was performed using one-way ANOVA with Dunnett's post-hoc test for control comparison and Newman-Keuls' post-hoc test for multiple comparisons between AgNP and AgNP:PVP results (***$p<0.001$, ###$p<0.001$, ‡‡‡$p<0.001$ and ‡$p<0.05$)

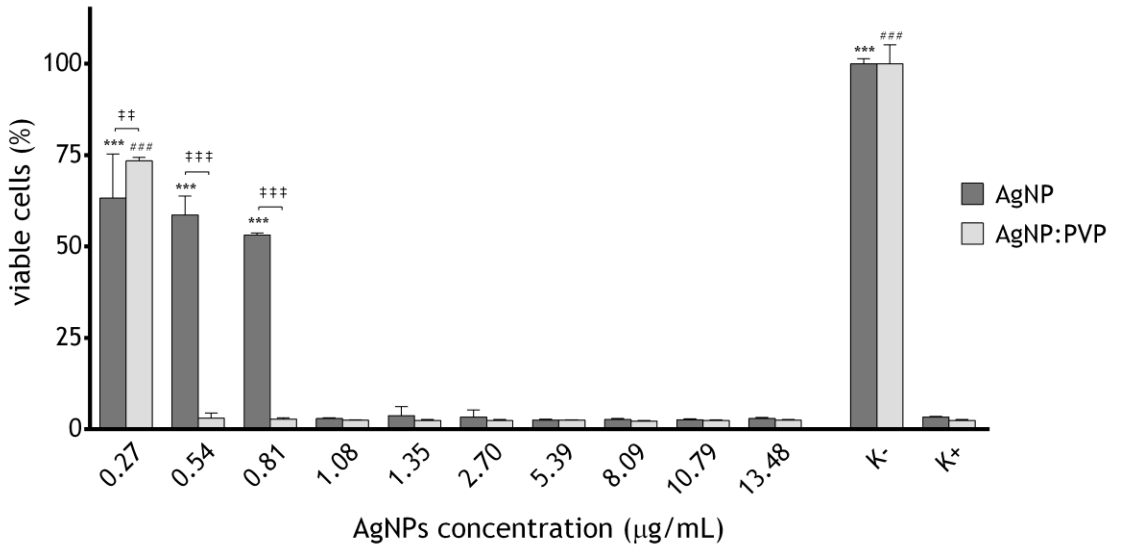

Figure 18 - Antifungal activity of two different types of nanoparticles produced for *T. mentagrophytes*. Negative control (K^-), positive control (K^+). Each result is mean ± standard error of the mean of at least three independent experiments. Statistical analysis was performed using one-way ANOVA with Dunnett's post-hoc test for control comparison and Newman-Keuls' post-hoc test for multiple comparisons between AgNP and AgNP:PVP results (***$p<0.001$, ###$p<0.001$, ‡‡‡$p<0.001$, ‡‡$p<0.01$).

Analyzing both figure 17 and figure 18, a few differences in the MIC results can be seen. Namely, the major antifungal property that AgNPs coated with PVP have compared to the AgNP alone. Their dispersion in solution and regular shape may lead to this improved activity, while the increased aggregation leads to the generation of spacious aggregates, with reduced surface area that would therefore reduce the interactions between nanoparticles and microorganism cells, leading to a loss of antimicrobial activity (Kvítek *et al.*, 2008; Rathod *et al.*, 2011; Zhou *et al.*, 2012). The values of MICs are resumed in the table 5. Analyzing them for the same fungal strain, a much higher value of AgNP is needed to kill the same quantity of microorganisms, relatively to AgNP:PVP. For instance, in *T. rubrum,* a value of 5.39 µg/mL of AgNP is needed to kill 90% of the strain and about half that value, 2.70 µg/mL of AgNP:PVP is enough to have the same effect. Also, comparing the two different strains, both AgNP and AgNP:PVP have an enhanced antimicrobial effect against *T. mentagrophytes*, meaning that this dermatophyte is more susceptible to the silver at a nanoscale than *T. rubrum*. All the MIC values obtained and presented in the table prove that.

Table 5 - Values of MIC obtained in this study.

Dermatophyte strain	Nanoparticles	MIC_{50} (µg/mL)	MIC_{90} (µg/mL)
Trichophyton rubrum	AgNP	1.35	5.39
	AgNP:PVP	0.81 - 0.54	2.70
Trichophyton mentagrophytes	AgNP	0.81	1.08
	AgNP:PVP	0.27 - 0.54	0.54

These results reveal that both AgNP intrinsic properties actually had effect on killing the two different strains of dermatophytes, using a low concentration. As previously reported in the literature, Marcato and colleagues tested *T. rubrum* and Kim and coworkers worked with *T. mentagrophytes* and calculated MICs of AgNPs for both strains. In the first study, values between 1 and 2 µg/mL allowed to kill 80% of the strain, showing their AgNPs significant antifungal activity (Marcato *et al.*, 2012). The second work showed a bigger interval of concentrations that inhibited the same 80% of growth, using 1 to 7 µg/mL of AgNPs (Kim *et al.*, 2008). There are other works in which MICs of 5 to 10 µg/mL for *T. rubrum* (Noorbakhsh *et al.*, 2011) and 2 µg/mL for *T. mentagrophytes* were obtained (Rathod *et al.*, 2011). More results are already published with other strains of fungi, such as the *Candida* genus, which are responsible for the candidiasis infections (Rodrigues *et al.*, 2013).

Relatively to other antifungal agents that are presented in table 6, the MIC values obtained in this study for AgNPs were higher than previously described in the literature,

meaning that a higher concentration of particles is needed to kill microorganisms. However, the MICs obtained for AgNP:PVP are quite promising, in comparison to that reported for AgNPs produced by other authors. This potential antifungal activity of silver may be even improved if used together with one of the antifungal referred below in the table.

Table 6 - Antifungal drugs susceptibility data for *T. rubrum* and *T. mentagrophytes* (da Silva Barros *et al.*, 2007).

Dermatophyte strain	Antifungal agent	MIC_{50} (μg/mL)	MIC_{90} (μg/mL)
Trichophyton rubrum	Fluconazole	16	32
	Itraconazole	0.062	0.250
	Griseofulvin	0.250	1
	Terbinafine	< 0.007	0.007
Trichophyton mentagrophytes	Fluconazole	32	64
	Itraconazole	0.006	0.125
	Griseofulvin	0.250	0.500
	Terbinafine	0.007	0.015

3.3. Characterization of the Nanoparticles Cytotoxic Profile

To evaluate if the nanoparticles produced have or not harmful side effects, keratinocytes were used as model cells to evaluate their cytotoxic profile. To ascertain this property, an assay was performed using either AgNP and AgNP:PVP that were added to cells.

The data reported in literature is ambiguous concerning the cytotoxic properties of AgNPs. Several articles refer that silver is cytotoxic for keratinocytes and consequently inhibits cell growth and proliferation (Poon and Burd, 2004; Paddle-Ledinek *et al.*, 2006; Atiyeh *et al.*, 2007; Zanette *et al.*, 2011). AgNPs' toxicity depends on the type of particles, size, shape, composition and functionalization, which can their interactions with cells. Moreover, the most important factor that can damage or not cells is the concentration of Ag used for particles production. It is expected that a higher concentration have a greater toxic effect on cells, as it does in microorganisms, such as the dermatophytes studied before. As described by Samberg and colleagues, AgNPs themselves may not be responsible for an increased cell mortality (Samberg *et al.*, 2010). It may be the excipients added to the particles that are responsible for their toxic effect. In this study, PVP was used to coat particles and this polymer was labelled before as non-toxic to keratinocytes, making it a good stabilizing agent (Lu *et al.*, 2010).

Through the analysis of figure 19 and 20, cell adhesion and proliferation can be observed in the negative control (K^-) where cells in a stretched and connected form can be seen, and conversely, the round and shrunken morphology of dead cells were verified in the positive control (K^+), where cells were intentionally killed with ethanol. In the same figures, it is possible to verify that cell death is proportional to AgNP and AgNP:PVP concentration increase. Cells in contact with the higher concentrations of AgNPs (10.79 µg/mL and 13.48 µg/mL) have a similar shape to that of K^+, revealing that silver have a toxic effect on them. However, in lower concentrations cells with a stretched form, which is typical of viable cells, are observed. This confirms the concentration-related cytotoxicity of silver (AshaRani *et al.*, 2008).

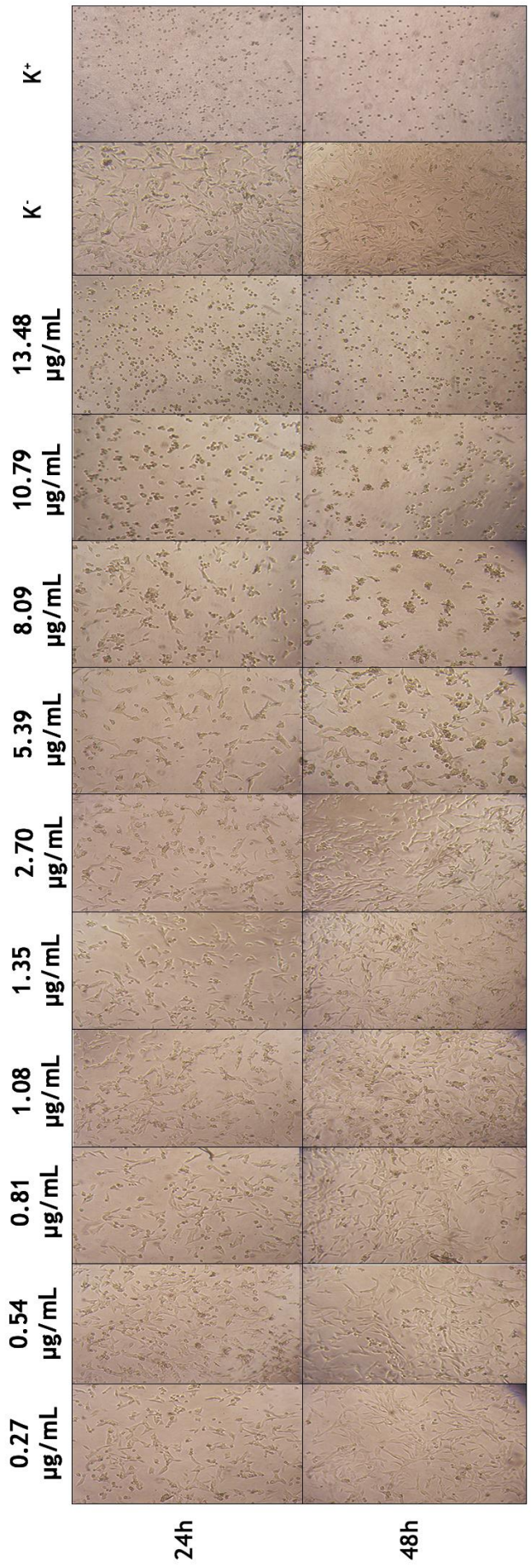

Figure 19 – Inverted light microscope images of keratinocytes in contact with different AgNP concentrations (indicated on top) and also in the negative control (living cells) and positive control (dead cells) at the two different times evaluated (24h and 48h).

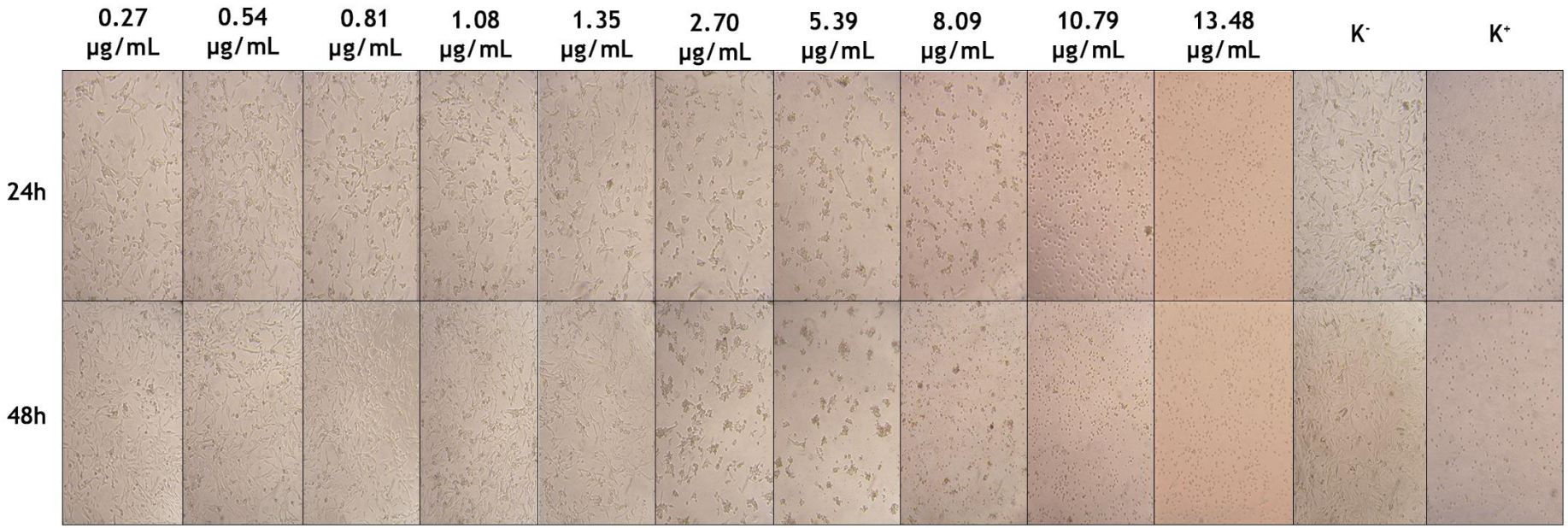

Figure 20 – Inverted light microscope images of keratinocytes in contact with different AgNP:PVP concentrations (indicated on top) and also in the negative control (living cells) and positive control (dead cells) at the two different times evaluated (24h and 48h).

Regarding the MTS assay, which allowed the quantification of viable cells and consequently the cytotoxic effect of the different AgNPs produced, figure 21 shows that the cell viability did not reach the same values obtained for the negative control, either at 24 or at 48h. This result may be explained by the fact that the particles do not possess any protecting agent. Therefore, the silver ions diffusion from AgNP towards the cells occurs more easily and therefore, some cytotoxic effect arises more quickly. Nevertheless, cell viability reach values about 75-80%, which do not substantially decrease in time, until AgNP concentrations higher than 8.09 µg/mL are used. Hence, from this value cell death occurs more predominately, with an increased toxic effect between 24 and 48h. This result indicates that AgNP have a harmful effect on keratinocytes at a minimum concentration of 8.09 µg/mL.

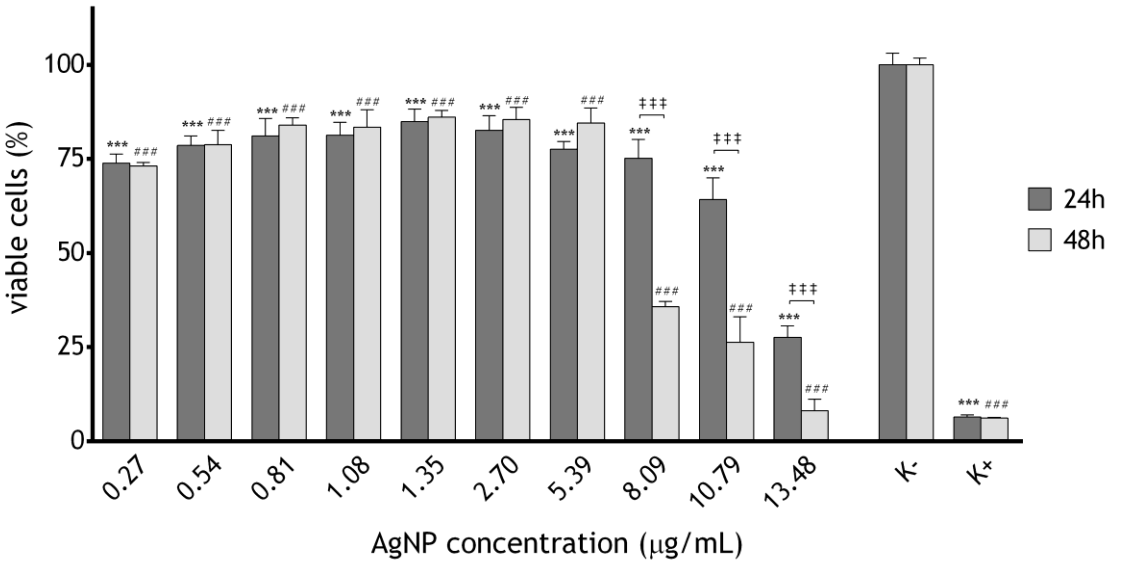

Figure 21 – Characterization of cellular viability when in contact with AgNP, measured by a MTS assay. Negative control (K^-), positive control (K^+). Each result is mean ± standard error of the mean of at least three independent experiments. Statistical analysis was performed using one-way ANOVA with Dunnett's post-hoc test for control comparisons and Newman-Keuls' post-hoc test for multiple comparisons between 24h and 48h results (***$p<0.001$, ###$p<0.001$, ‡‡‡$p<0.001$).

Relatively to the other prepared nanoparticles, AgNP:PVP, the MTS assay results presented in figure 22 revealed that for lower concentrations of nanoparticles, cells presented a viability around 100%, at 24 and 48h. The rise in cell death occurs at 24h when the silver concentration 5.39 µg/mL was used but as the time increases and reaches the 48h, a lower concentration is enough to induce toxic effects on keratinocytes. For instance, a value of 75% of viable cells corresponds to 5.39 µg/mL at 24h of incubation, but after 48h the concentration decreases to half, 2.70 µg/mL.

The polymer coating seems to be responsible for a delayed effect, since the exposure of silver positive ions presented in the nanoparticle to cell membranes is not as intense as the previous AgNP due to PVP coating. Herewith, cell adhesion, growth and proliferation in a short time will therefore be higher with these AgNP:PVP. However, in a long-term AgNP:PVP revealed to be more cytotoxic than AgNP alone. An explanation for this event is that although the PVP protect cells from ion diffusion, this polymer also lead to a better size, shape and dispersion of the nanoparticles. Therefore, AgNP:PVP have an improved effect also against KEC cells. This result is consistent with what happened before with AgNPs antifungal activity. AgNP:PVP present a larger surface area to volume ratio, while AgNP are subjected to particles self-interaction and further agglomeration, which reduces its capacity to damage cells.

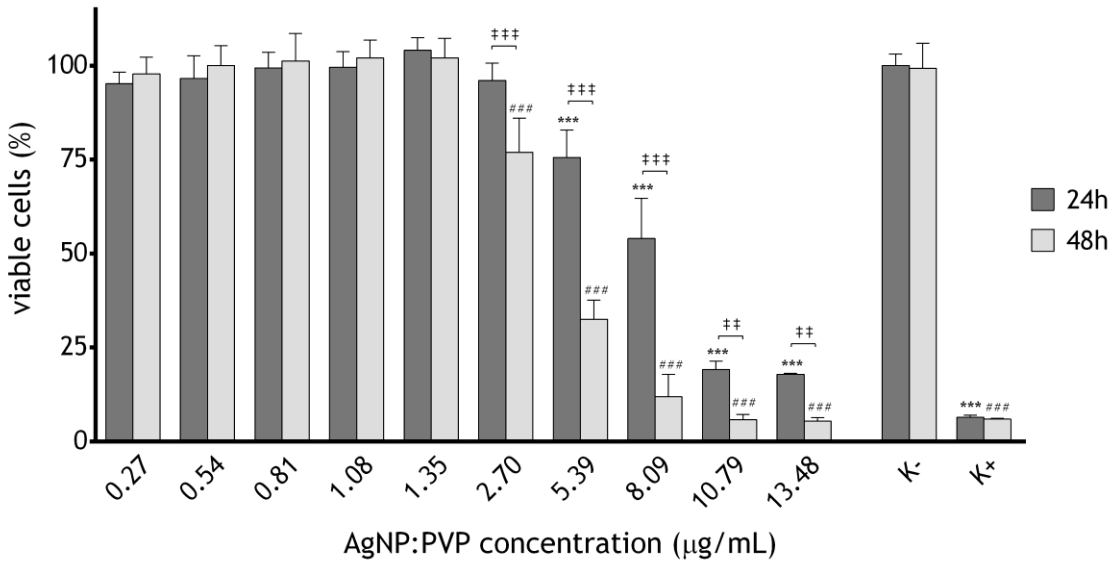

Figure 22 – Characterization of cellular viability when in contact with AgNP:PVP, measured by a MTS assay. Negative control (K^-), positive control (K^+). Each result is mean ± standard error of the mean of at least three independent experiments. Statistical analysis was performed using one-way ANOVA with Dunnett's post-hoc test for control comparisons and Newman-Keuls' post-hoc test for multiple comparisons between 24h and 48h results (***$p<0.001$, ###$p<0.001$, ‡‡‡$p<0.001$, ‡‡$p<0.01$).

Still, a crucial point in this investigation was to compare cytotoxicity to both pathogenic microorganisms and to skin cells. The results obtained revealed that the two different nanoparticles produced, AgNP and AgNP:PVP, are more toxic to either *T. rubrum* or *T. mentagrophytes* than to the keratinocyte cells from the epidermal layer of the skin. This effect was previously described in the literature (Chen *et al.*, 2011) and makes AgNPs, in particular AgNP:PVP, a potential nanomaterial to fight against dermatophyte infections that affect skin, nails and hair, causing trouble to millions of people around the world.

Chapter IV

CONCLUSION and FUTURE PERSPECTIVES

4. Conclusion and Future Perspectives

Silver is known for a long time for its antimicrobial activity. However, it has been essentially applied in antibacterial applications, leaving thus the antifungal properties on the back burner. Taking advantage from the silver properties, in the present study, silver nanoparticles were prepared for being used against infections caused by dermatophytes in the epidermis. Such infections are mainly caused by two different strains: *Trichophyton rubrum* and *Trichophyton mentagrophytes*.

Herein, AgNPs were prepared by using a chemical reduction method and consequently, an extensive characterization of the produced nanoparticles was performed. The UV-Vis results confirmed the presence of AgNPs in solution while FTIR, XRD and EDX were used to evaluate the different chemical properties of the particles. SEM was very useful to verify the morphology of both AgNP and AgNP:PVP, although due to the small size of the nanoparticles (≈ 40 nm of average diameter), the images obtained had a limited definition.

Furthermore, MIC assays were done to evaluate the antifungal activity of the prepared nanoparticles against the two dermatophyte strains studied. The results showed that AgNP:PVP had a higher potential to be used against fungal infections. Particles cytotoxic profile was evaluated by using keratinocytes, which are the typical cells that are found in the stratum corneum affected by fungal invasions. Through *in vitro* studies, more precisely, a MTS assay, the cytotoxicity associated to both AgNPs produced was evaluated, and it showed that AgNP:PVP had no effect on cells when low concentrations were used, allowing its adhesion, growth and proliferation of eukaryotic cells. Nonetheless, in higher concentrations the particles had a harmful effect for keratinocytes. Still, there are concentrations in which AgNP:PVP kill microbial cells and do not harm the mammalian cells, which was the main goal of this study and was successfully accomplished.

In a futuristic perspective, other characterization techniques would be interesting to perform, allowing to get a deeper idea about the nanoparticles properties. Methods such as TEM are more suitable to observe small particles with a better resolution. Also, with this technique it would be plausible to verify the interactions between nanoparticles and microorganisms with a high magnification. Another technique that is useful when dealing with nanotechnology is the dynamic light scattering (DLS), which is a procedure used to determine the size distribution profile of particles in solution, but that is not available in the research centre where this work was developed.

Moreover, there are several ideas to carry on based on the work developed in this master thesis. After preparing, characterizing and evaluating both antifungal potential and cytotoxic profile, the resulting nanoparticles should be allocated in another material to easily reach the main target site of a possible skin infection. For instance, a hydrogel with intrinsic antimicrobial properties that together with AgNPs may have improved antifungal activities.

Other example of a possible material that may host the produced nanoparticles is a membrane of nanofibers, which could act as a patch in the local of the infection.

Also, a crucial point to be further investigated would be *in vivo* assays to evaluate the evolution of the infection when in contact with the biomaterial, being thus possible to confirm the potential of the hydrogel/membrane loaded with silver nanoparticles for medical applications.

Chapter V

BIBLIOGRAPHY

5. Bibliography

Acosta-Torres, L.S., Mendieta, I., Nuñez-Anita, R.E., Cajero-Juárez, M. and Castaño, V.M., 2012. *Cytocompatible antifungal acrylic resin containing silver nanoparticles for dentures*. International Journal of Nanomedicine, 7: 4777-4786.

Agnihotri, S., Mukherji, S. and Mukherji, S., 2012. *Antimicrobial chitosan-PVA hydrogel as a nanoreactor and immobilizing matrix for silver nanoparticles*. Applied Nanoscience, 2: 179-188.

Albanese, A., Tang, P.S. and Chan, W.C., 2012. *The effect of nanoparticle size, shape, and surface chemistry on biological systems*. Annual Review of Biomedical Engineering, 14: 1-16.

Alexander, J.W., 2009. *History of the medical use of silver*. Surgical Infections, 10: 289-292.

Allhoff, F. and Lin, P., 2010. *What's so special about nanotechnology and nanoethics?* International Journal of Applied Philosophy, 20: 179-190.

Aruguete, D.M., Kim, B., Hochella, M.F., Ma, Y., Cheng, Y., Hoegh, A., Liu, J. and Pruden, A., 2013. *Antimicrobial nanotechnology: its potential for the effective management of microbial drug resistance and implications for research needs in microbial nanotoxicology*. Environmental Science: Processes & Impacts, 15: 93-102.

AshaRani, P.V., Low Kah Mun, G., Hande, M.P. and Valiyaveettil, S., 2008. *Cytotoxicity and genotoxicity of silver nanoparticles in human cells*. ACS Nano, 3: 279-290.

Atiyeh, B.S., Costagliola, M., Hayek, S.N. and Dibo, S.A., 2007. *Effect of silver on burn wound infection control and healing: review of the literature*. Burns, 33: 139-148.

Baldo, A., Monod, M., Mathy, A., Cambier, L., Bagut, E.T., Defaweux, V., Symoens, F., Antoine, N. and Mignon, B., 2012. *Mechanisms of skin adherence and invasion by dermatophytes*. Mycoses, 55: 218-223.

Bin Ahmad, M., Lim, J.J., Shameli, K., Ibrahim, N.A., Tay, M.Y. and Chieng, B.W., 2012. *Antibacterial activity of silver bionanocomposites synthesized by chemical reduction route*. Chemistry Central Journal, 6: 101.

Blanpain, C. and Fuchs, E., 2009. *Epidermal homeostasis: a balancing act of stem cells in the skin*. Nature Reviews Molecular Cell Biology, 10: 207-217.

Bryaskova, R., Pencheva, D., Nikolov, S. and Kantardjiev, T., 2011. *Synthesis and comparative study on the antimicrobial activity of hybrid materials based on silver nanoparticles (AgNps) stabilized by polyvinylpyrrolidone (PVP)*. Journal of Chemical Biology, 4: 185-191.

Chaloupka, K., Malam, Y. and Seifalian, A.M., 2010. *Nanosilver as a new generation of nanoproduct in biomedical applications*. Trends in Biotechnology, 28: 580-588.

Charles, A.J., 2009. *Superficial cutaneous fungal infections in tropical countries*. Dermatologic Therapy, 22: 550-559.

Chen, M., Yang, Z., Wu, H., Pan, X., Xie, X. and Wu, C., 2011. *Antimicrobial activity and the mechanism of silver nanoparticle thermosensitive gel*. International Journal of Nanomedicine, 6: 2873-2877.

Chen, X. and Schluesener, H.J., 2008. *Nanosilver: a nanoproduct in medical application*. Toxicology Letters, 176: 1-12.

Clark, R.A., Ghosh, K. and Tonnesen, M.G., 2007. *Tissue engineering for cutaneous wounds*. Journal of Investigative Dermatology, 127: 1018-1029.

CLSI, 2008. *Reference Method for Broth Dilution Antifungal Susceptibility Testing of Filamentous Fungi; Approved Standard-Second Edition*. CLSI document M38-A2. Clinical and Laboratory Standards Institute, 28: 1-35.

da Silva Barros, M.E., de Assis Santos, D. and Hamdan, J.S., 2007. *Evaluation of susceptibility of Trichophyton mentagrophytes and Trichophyton rubrum clinical isolates to antifungal drugs using a modified CLSI microdilution method (M38-A)*. Journal of Medical Microbiology, 56: 514-518.

de Souza, A.L.R., Kiill, C.P., dos Santos, F.K., da Luz, G.M., Silva, H.R.E., Chorilli, M. and Gremião, M.P.D., 2012. *Nanotechnology-based drug delivery systems for dermatomycosis treatment*. Current Nanoscience, 8: 512-519.

Deivaraj, T.C., Lala, N.L. and Lee, J.Y., 2005. *Solvent-induced shape evolution of PVP protected spherical silver nanoparticles into triangular nanoplates and nanorods*. Journal of Colloid and Interface Science, 289: 402-409.

Desai, R., Mankad, V., Gupta, S.K. and Jha, P.K., 2012. *Size distribution of silver nanoparticles: UV-visible spectroscopic assessment*. Nanoscience and Nanotechnology Letters, 4: 30-34.

El Badawy, A.M., Luxton, T.P., Silva, R.G., Scheckel, K.G., Suidan, M.T. and Tolaymat, T.M., 2010. *Impact of environmental conditions (pH, ionic strength, and electrolyte type) on the surface charge and aggregation of silver nanoparticles suspensions*. Environmental Science & Technology, 44: 1260-1266.

Gajbhiye, M., Kesharwani, J., Ingle, A., Gade, A. and Rai, M., 2009. *Fungus-mediated synthesis of silver nanoparticles and their activity against pathogenic fungi in combination with fluconazole*. Nanomedicine: Nanotechnology, Biology, and Medicine, 5: 382-386.

Galdiero, S., Falanga, A., Vitiello, M., Cantisani, M., Marra, V. and Galdiero, M., 2011. *Silver nanoparticles as potential antiviral agents*. Molecules, 16: 8894-8918.

García-Barrasa, J., López-de-Luzuriaga, J.M. and Monge, M., 2010. *Silver nanoparticles: synthesis through chemical methods in solution and biomedical applications*. Central European Journal of Chemistry, 9: 7-19.

Gaspar, V.M., Correia, I.J., Sousa, A., Silva, F., Paquete, C.M., Queiroz, J.A. and Sousa, F., 2011a. *Nanoparticle mediated delivery of pure P53 supercoiled plasmid DNA for gene therapy*. Journal of Controlled Release, 156: 212-222.

Gaspar, V.M., Sousa, F., Queiroz, J.A. and Correia, I.J., 2011b. *Formulation of chitosan-TPP-pDNA nanocapsules for gene therapy applications*. Nanotechnology, 22: 015101.

Ghannoum, M.A., Chaturvedi, V., Espinel-Ingroff, A., Pfaller, M.A., Rinaldi, M.G., Lee-Yang, W. and Warnock, D.W., 2004. *Intra- and interlaboratory study of a method for testing the antifungal susceptibilities of dermatophytes*. Journal of Clinical Microbiology, 42: 2977-2979.

Goldstein, J.I., Newbury, D.E., Joy, D.C., Lyman, C.E., Echlin, P., Lifshin, E., Sawyer, L. and Michael, J.R., 2003. *X-Ray Spectral Measurement: EDS and WDS*. In *Scanning electron microscopy and X-ray microanalysis*. Springer, 7: 297-353.

Gong, P., Li, H., He, X., Wang, K., Hu, J., Tan, W., Zhang, S. and Yang, X., 2007. *Preparation and antibacterial activity of Fe3O4@Ag nanoparticles*. Nanotechnology, 18: 285604.

Gordon, O., Vig Slenters, T., Brunetto, P.S., Villaruz, A.E., Sturdevant, D.E., Otto, M., Landmann, R. and Fromm, K.M., 2010. *Silver coordination polymers for prevention of implant infection: thiol interaction, impact on respiratory chain enzymes, and hydroxyl radical induction*. Antimicrobial Agents and Chemotherapy, 54: 4208-4218.

Gorup, L.F., Longo, E., Leite, E.R. and Camargo, E.R., 2011. *Moderating effect of ammonia on particle growth and stability of quasi-monodisperse silver nanoparticles synthesized by the Turkevich method*. Journal of Colloid and Interface Science, 360: 355-358.

Grade, S., Eberhard, J., Neumeister, A., Wagener, P., Winkel, A., Stiesch, M. and Barcikowski, S., 2012. *Serum albumin reduces the antibacterial and cytotoxic effects of hydrogel-embedded colloidal silver nanoparticles*. RSC Advances, 2: 7190-7196.

Gupta, A.K. and Cooper, E.A., 2008. *Update in antifungal therapy of dermatophytosis*. Mycopathologia, 166: 353-367.

Havlickova, B., Czaika, V.A. and Friedrich, M., 2008. *Epidemiological trends in skin mycoses worldwide*. Mycoses, 51: 2-15.

Hussain, J.I., Kumar, S., Hashmi, A.A. and Khan, Z., 2011. *Silver nanoparticles: preparation, characterization, and kinetics*. Advanced Materials Letters, 2: 188-194.

Jain, J., Arora, S., Rajwade, J.M., Omray, P., Khandelwal, S. and Paknikar, K.M., 2009. *Silver nanoparticles in therapeutics: development of an antimicrobial gel formulation for topical use*. Molecular Pharmaceutics, 6: 1388-1401.

Jessup, C.J., Warner, J., Isham, N., Hasan, I. and Ghannoum, M.A., 2000. *Antifungal susceptibility testing of dermatophytes: establishing a medium for inducing conidial growth and evaluation of susceptibility of clinical isolates*. Journal of Clinical Microbiology, 38: 341-344.

Jia, Q., Shan, S., Jiang, L., Wang, Y. and Li, D., 2012. *Synergistic antimicrobial effects of polyaniline combined with silver nanoparticles*. Journal of Applied Polymer Science, 125: 3560-3566.

Jiang, X. and Yu, A., 2010. *One-Step approach for the synthesis and self-assembly of silver nanoparticles*. Journal of Nanoscience and Nanotechnology, 10: 7643-7647.

Khan, Z., Al-Thabaiti, S.A., Obaid, A.Y. and Al-Youbi, A.O., 2011. *Preparation and characterization of silver nanoparticles by chemical reduction method*. Colloids and Surfaces B: Biointerfaces, 82: 513-517.

Khatoon, U.T., Rao, K.V., Rao, J.V.R. and Aparna, Y., 2011. *Synthesis and characterization of silver nanoparticles by chemical reduction method*. International Conference on Nanoscience, Engineering and Technology (ICONSET): 97-99.

Kim, J.S., Kuk, E., Yu, K.N., Kim, J.H., Park, S.J., Lee, H.J., Kim, S.H., Park, Y.K., Park, Y.H., Hwang, C.Y., Kim, Y.K., Lee, Y.S., Jeong, D.H. and Cho, M.H., 2007. *Antimicrobial effects of silver nanoparticles*. Nanomedicine: Nanotechnology, Biology, and Medicine, 3: 95-101.

Kim, K.J., Sung, W.S., Moon, S.K., Choi, J.S., Kim, J.G. and Lee, D.G., 2008. *Antifungal effect of silver nanoparticles on dermatophytes*. Journal of Microbiology and Biotechnology, 18: 1482-1484.

Kim, K.J., Sung, W.S., Suh, B.K., Moon, S.K., Choi, J.S., Kim, J.G. and Lee, D.G., 2009. *Antifungal activity and mode of action of silver nano-particles on Candida albicans*. Biometals, 22: 235-242.

Kim, Y., Suh, H.S., Cha, H.J., Kim, S.H., Jeong, K.S. and Kim, D.H., 2009. *A case of generalized argyria after ingestion of colloidal silver solution*. American Journal of Industrial Medicine, 52: 246-250.

Krishnaraj, C., Ramachandran, R., Mohan, K. and Kalaichelvan, P.T., 2012. *Optimization for rapid synthesis of silver nanoparticles and its effect on phytopathogenic fungi*. Spectrochimica Acta Part A: Molecular and Biomolecular Spectroscopy, 93: 95-99.

Kvítek, L., Panáček, A., Soukupová, J., Kolář, M., Večeřová, R., Prucek, R., Holecová, M. and Zbořil, R., 2008. *Effect of surfactants and polymers on stability and antibacterial activity of silver nanoparticles (NPs)*. Journal of Physical Chemistry C, 112: 5825-5834.

Kyle, A.A. and Dahl, M.V., 2004. *Topical therapy for fungal infections*. American Journal of Clinical Dermatology, 5: 443-451.

Lawrie, G., Keen, I., Drew, B., Chandler-Temple, A., Rintoul, L., Fredericks, P. and Grøndahl, L., 2007. *Interactions between alginate and chitosan biopolymers characterized using FTIR and XPS*. Biomacromolecules, 8: 2533-2541.

Leaper, D.J., 2006. *Silver dressings: their role in wound management*. International Wound Journal, 3: 282-294.

Lee, J., Kim, K.J., Sung, W.S., Kim, J.G. and Lee, D.G., 2008. *The Silver Nanoparticle (Nano-Ag): a New Model for Antifungal Agents*. In *Silver Nanoparticles*, Perez, D.P., (Ed.). 15: 295-308.

Lee, S.M., Song, K.C. and Lee, B.S., 2010. *Antibacterial activity of silver nanoparticles prepared by a chemical reduction method*. Korean Journal of Chemical Engineering, 27: 688-692.

Li, G., Wen, Q., Zhang, T. and Ju, Y., 2013. *Synthesis and properties of silver nanoparticles in chitosan-based thermosensitive semi-interpenetrating hydrogels*. Journal of Applied Polymer Science, 127: 2690-2697.

Li, W.R., Xie, X.B., Shi, Q.S., Duan, S.S., Ouyang, Y.S. and Chen, Y.B., 2011. *Antibacterial effect of silver nanoparticles on Staphylococcus aureus*. Biometals, 24: 135-141.

Lok, C.N., Ho, C.M., Chen, R., He, Q.Y., Yu, W.Y., Sun, H., Tam, P.K., Chiu, J.F. and Che, C.M., 2006. *Proteomic analysis of the mode of antibacterial action of silver nanoparticles*. Journal of Proteome Research, 5: 916-924.

Lu, S., Gao, W. and Gu, H.Y., 2008. *Construction, application and biosafety of silver nanocrystalline chitosan wound dressing*. Burns, 34: 623-628.

Lu, W., Senapati, D., Wang, S., Tovmachenko, O., Singh, A.K., Yu, H. and Ray, P.C., 2010. *Effect of surface coating on the toxicity of silver nanomaterials on human skin keratinocytes*. Chemical Physics Letters, 487: 92-96.

Madison, K.C., 2003. *Barrier function of the skin: "la raison d'être" of the epidermis*. Journal of Investigative Dermatology, 121: 231-241.

Maneerung, T., Tokura, S. and Rujiravanit, R., 2008. *Impregnation of silver nanoparticles into bacterial cellulose for antimicrobial wound dressing*. Carbohydrate Polymers, 72: 43-51.

Marcato, P.D., Durán, M., Huber, S.C., Rai, M., Melo, P.S., Alves, O.L. and Durán, N., 2012. *Biogenic silver nanoparticles and its antifungal activity as a new topical transungual drug*. Journal of Nano Research, 20: 99-107.

Mayser, P.P.M. and Gräser, Y., 2011. *Superficial Fungal Infections*. In *Harper's Textbook of Pediatric Dermatology, Volume 1, 2, Third Edition*, Irvine, A.D., Hoeger, P.H. and Yan, A.C., (Eds.). Wiley-Blackwell, 62: 62.61-62.34.

Metcalfe, A.D. and Ferguson, M.W., 2007. *Bioengineering skin using mechanisms of regeneration and repair*. Biomaterials, 28: 5100-5113.

Monteiro, D.R., Gorup, L.F., Silva, S., Negri, M., de Camargo, E.R., Oliveira, R., Barbosa, D.B. and Henriques, M., 2011. *Silver colloidal nanoparticles: antifungal effect against adhered cells and biofilms of Candida albicans and Candida glabrata*. Biofouling, 27: 711-719.

Monteiro, D.R., Gorup, L.F., Takamiya, A.S., Ruvollo-Filho, A.C., de Camargo, E.R. and Barbosa, D.B., 2009. *The growing importance of materials that prevent microbial adhesion: antimicrobial effect of medical devices containing silver*. International Journal of Antimicrobial Agents, 34: 103-110.

Morales-Sánchez, J.E., Guajardo-Pacheco, J., Noriega-Treviño, M., Quintero-González, C., Compeán-Jasso, M., López-Salinas, F., González-Hernández, J. and Ruiz, F., 2011. *Synthesis of silver nanoparticles using albumin as a reducing agent*. Materials Sciences and Applications, 2: 578-581.

Moriarty, B., Hay, R. and Morris-Jones, R., 2012. *The diagnosis and management of tinea*. BMJ, 345: e4380.

Morones, J.R., Elechiguerra, J.L., Camacho, A., Holt, K., Kouri, J.B., Ramírez, J.T. and Yacaman, M.J., 2005. *The bactericidal effect of silver nanoparticles*. Nanotechnology, 16: 2346-2353.

Naik, R.R., Stringer, S.J., Agarwal, G., Jones, S.E. and Stone, M.O., 2002. *Biomimetic synthesis and patterning of silver nanoparticles*. Nature Materials, 1: 169-172.

Nguyen, V.H., Kim, B.K., Jo, Y.L. and Shim, J.J., 2012. *Preparation and antibacterial activity of silver nanoparticles-decorated graphene composites*. The Journal of Supercritical Fluids, 72: 28-35.

Noorbakhsh, F., Rezaie, S. and Shahverdi, A.R., 2011. *Antifungal effects of silver nanoparticle alone and with combination of antifungal drug on dermatophyte pathogen Trichophyton rubrum*. International Conference of Bioscience, Biochemistry and Bioinformatics, 5: 264-267.

O'Brien, J., Wilson, I., Orton, T. and Pognan, F., 2000. *Investigation of the Alamar Blue (resazurin) fluorescent dye for the assessment of mammalian cell cytotoxicity*. European Journal of Biochemistry, 267: 5421-5426.

Paddle-Ledinek, J.E., Nasa, Z. and Cleland, H.J., 2006. *Effect of different wound dressings on cell viability and proliferation*. Plastic and Reconstructive Surgery, 117: 110S-118S.

Panáček, A., Kolář, M., Večeřová, R., Prucek, R., Soukupová, J., Kryštof, V., Hamal, P., Zbořil, R. and Kvítek, L., 2009. *Antifungal activity of silver nanoparticles against Candida spp*. Biomaterials, 30: 6333-6340.

Phukon, P., Saikia, J.P. and Konwar, B.K., 2011. *Enhancing the stability of colloidal silver nanoparticles using polyhydroxyalkanoates (PHA) from Bacillus circulans (MTCC 8167) isolated from crude oil contaminated soil*. Colloids and Surfaces B: Biointerfaces, 86: 314-318.

Polte, J., Tuaev, X., Wuithschick, M., Fischer, A., Thuenemann, A.F., Rademann, K., Kraehnert, R. and Emmerling, F., 2012. *Formation mechanism of colloidal silver nanoparticles: analogies and differences to the growth of gold nanoparticles*. ACS Nano, 6: 5791-5802.

Poon, V.K. and Burd, A., 2004. *In vitro cytotoxity of silver: implication for clinical wound care*. Burns, 30: 140-147.

Prow, T.W., Grice, J.E., Lin, L.L., Faye, R., Butler, M., Becker, W., Wurm, E.M., Yoong, C., Robertson, T.A., Soyer, H.P. and Roberts, M.S., 2011. *Nanoparticles and microparticles for skin drug delivery*. Advanced Drug Delivery Reviews, 63: 470-491.

Puchalski, M., Dąbrowski, P., Olejniczak, W., Krukowski, P., Kowalczyk, P. and Polański, K., 2007. *The study of silver nanoparticles by scanning electron microscopy, energy dispersive X-ray analysis and scanning tunnelling microscopy*. Materials Science-Poland, 25: 473-478.

Raffi, M., Hussain, F., Bhatti, T.M., Akhter, J.I., Hameed, A. and Hasan, M.M., 2008. *Antibacterial characterization of silver nanoparticles against E. coli ATCC-15224*. Journal of Materials Science and Technology, 24: 192-196.

Rai, M., Yadav, A. and Gade, A., 2009. *Silver nanoparticles as a new generation of antimicrobials*. Biotechnology Advances, 27: 76-83.

Raje, V.P., Morgado, P.I., Ribeiro, M.P., Correia, I.J., Bonifácio, V.D., Branco, P.S. and Aguiar-Ricardo, A., 2013. *Dual on-off and off-on switchable oligoaziridine biosensor*. Biosensors and Bioelectronics, 39: 64-69.

Rathod, V., Banu, A. and Ranganath, E., 2011. *Biosynthesis of highly stabilized silver nanoparticles by Rhizopus stolonifer and their Anti-fungal efficacy*. International Journal of Molecular and Clinical Microbiology, 1: 65-70.

Ravishankar Rai, V. and Jumuna Bai, A., 2011. *Nanoparticles and their potential applications as antimicrobials*. Science Against Microbial Pathogens, 1: 197-209.

Ribeiro, M.P., Espiga, A., Silva, D., Baptista, P., Henriques, J., Ferreira, C., Silva, J.C., Borges, J.P., Pires, E., Chaves, P. and Correia, I.J., 2009. *Development of a new chitosan hydrogel for wound dressing*. Wound Repair and Regeneration, 17: 817-824.

Rodrigues, A.G., Ping, L.Y., Marcato, P.D., Alves, O.L., Silva, M.C., Ruiz, R.C., Melo, I.S., Tasic, L. and De Souza, A.O., 2013. *Biogenic antimicrobial silver nanoparticles produced by fungi*. Applied Microbiology and Biotechnology, 97: 775-782.

Ruparelia, J.P., Chatterjee, A.K., Duttagupta, S.P. and Mukherji, S., 2008. *Strain specificity in antimicrobial activity of silver and copper nanoparticles*. Acta Biomaterialia, 4: 707-716.

Ryder, N.S., 1992. *Terbinafine: mode of action and properties of the squalene epoxidase inhibition*. British Journal of Dermatology, 126: 2-7.

Sachs, D.L. and Voorhees, J.J., 2011. *Age-reversing drugs and devices in dermatology*. Clinical Pharmacology and Therapeutics, 89: 34-43.

Sadeghi, B., Jamali, M., Kia, S., Amininia, A. and Ghafari, S., 2010. *Synthesis and characterization of silver nanoparticles for antibacterial activity*. International Journal of Nano Dimension, 1: 119-124.

Samberg, M.E., Oldenburg, S.J. and Monteiro-Riviere, N.A., 2010. *Evaluation of silver nanoparticle toxicity in skin in vivo and keratinocytes in vitro*. Environmental Health Perspectives, 118: 407-413.

Seil, J.T. and Webster, T.J., 2012. *Antimicrobial applications of nanotechnology: methods and literature*. International Journal of Nanomedicine, 7: 2767-2781.

Seoudi, R., Shabaka, A., El Sayed, Z.A. and Anis, B., 2011. *Effect of stabilizing agent on the morphology and optical properties of silver nanoparticles*. Physica E: Low-dimensional Systems and Nanostructures, 44: 440-447.

Shahverdi, A.R., Fakhimi, A., Shahverdi, H.R. and Minaian, S., 2007. *Synthesis and effect of silver nanoparticles on the antibacterial activity of different antibiotics against Staphylococcus aureus and Escherichia coli*. Nanomedicine: Nanotechnology, Biology, and Medicine, 3: 168-171.

Shin, H.S., Yang, H.J., Kim, S.B. and Lee, M.S., 2004. *Mechanism of growth of colloidal silver nanoparticles stabilized by polyvinyl pyrrolidone in gamma-irradiated silver nitrate solution*. Journal of Colloid and Interface Science, 274: 89-94.

Silver, S., 2003. *Bacterial silver resistance: molecular biology and uses and misuses of silver compounds*. FEMS Microbiology Reviews, 27: 341-353.

Singal, A., 2008. *Butenafine and superficial mycoses: current status*. Expert Opinion on Drug Metabolism & Toxicology, 4: 999-1005.

Singh, A.K. and Raykar, V.S., 2008. *Microwave synthesis of silver nanofluids with polyvinylpyrrolidone (PVP) and their transport properties*. Colloid and Polymer Science, 286: 1667-1673.

Singh, C., Baboota, R.K., Naik, P.K. and Singh, H., 2012. *Biocompatible synthesis of silver and gold nanoparticles using leaf extract of Dalbergia sissoo*. Advanced Materials Letters, 3: 279-285.

Singh, M., Kumar, M., Kalaivani, R., Manikandan, S. and Kumaraguru, A.K., 2013. *Metallic silver nanoparticle: a therapeutic agent in combination with antifungal drug against human fungal pathogen*. Bioprocess and Biosystems Engineering, 36: 407-415.

Smith, B.C., 2011. *Fundamentals of Fourier Transform Infrared Spectroscopy*. CRC press, 1, 2: 1-53.

Sobczak-Kupiec, A., Malina, D., Kijkowska, R. and Wzorek, Z., 2012. *Influence of different types of stabilisers on the properties of silver nanoparticles suspension*. Micro & Nano Letters, 7: 818-821.

Song, K.C., Lee, S.M., Park, T.S. and Lee, B.S., 2009. *Preparation of colloidal silver nanoparticles by chemical reduction method*. Korean Journal of Chemical Engineering, 26: 153-155.

Van Dong, P., Ha, C., Binh, L.T. and Kasbohm, J., 2012. *Chemical synthesis and antibacterial activity of novel-shaped silver nanoparticles*. International Nano Letters, 2: 9.

Vasilev, K., Sah, V.R., Goreham, R.V., Ndi, C., Short, R.D. and Griesser, H.J., 2010. *Antibacterial surfaces by adsorptive binding of polyvinyl-sulphonate-stabilized silver nanoparticles*. Nanotechnology, 21: 215102.

Vermout, S., Tabart, J., Baldo, A., Mathy, A., Losson, B. and Mignon, B., 2008. *Pathogenesis of dermatophytosis*. Mycopathologia, 166: 267-275.

Vertelov, G.K., Krutyakov, Y.A., Efremenkova, O.V., Olenin, A.Y. and Lisichkin, G.V., 2008. *A versatile synthesis of highly bactericidal Myramistin(R) stabilized silver nanoparticles*. Nanotechnology, 19: 355707.

Vijayakumar, M., Priya, K., Nancy, F.T., Noorlidah, A. and Ahmed, A.B.A., 2013. *Biosynthesis, characterisation and anti-bacterial effect of plant-mediated silver nanoparticles using Artemisia nilagirica*. Industrial Crops and Products, 41: 235-240.

Wang, H., Qiao, X., Chen, J., Wang, X. and Ding, S., 2005. *Mechanisms of PVP in the preparation of silver nanoparticles*. Materials Chemistry and Physics, 94: 449-453.

Wong, K.K.Y. and Liu, X., 2013. *Nanotechnology meets regenerative medicine: a new frontier?* Nanotechnology Reviews, 2: 59-71.

Xu, Y., Gao, C., Li, X., He, Y., Zhou, L., Pang, G. and Sun, S., 2013. *In vitro antifungal activity of silver nanoparticles against ocular pathogenic filamentous fungi*. Journal of Ocular Pharmacology and Therapeutics, 29: 270-274.

Yamada, S., Sugahara, K. and Özbek, S., 2011. *Evolution of glycosaminoglycans: comparative biochemical study*. Communicative & Integrative Biology, 4: 150-158.

Yen, H.J., Hsu, S.H. and Tsai, C.L., 2009. *Cytotoxicity and immunological response of gold and silver nanoparticles of different sizes*. Small, 5: 1553-1561.

Yildirimer, L., Thanh, N.T. and Seifalian, A.M., 2012. *Skin regeneration scaffolds: a multimodal bottom-up approach*. Trends in Biotechnology, 30: 638-648.

Zaidi, Z. and Lanigan, S.W., 2010. *Skin: Structure and Function*. In *Dermatology in Clinical Practice*. Springer, 1: 1-15.

Zanette, C., Pelin, M., Crosera, M., Adami, G., Bovenzi, M., Larese, F.F. and Florio, C., 2011. *Silver nanoparticles exert a long-lasting antiproliferative effect on human keratinocyte HaCaT cell line*. Toxicology in Vitro, 25: 1053-1060.

Zhang, Q., Li, N., Goebl, J., Lu, Z. and Yin, Y., 2011. *A systematic study of the synthesis of silver nanoplates: is citrate a "magic" reagent?* Journal of the American Chemical Society, 133: 18931-18939.

Zhang, Z. and Michniak-Kohn, B.B., 2012. *Tissue engineered human skin equivalents*. Pharmaceutics, 4: 26-41.

Zhao, T., Sun, R., Yu, S., Zhang, Z., Zhou, L., Huang, H. and Du, R., 2010. *Size-controlled preparation of silver nanoparticles by a modified polyol method*. Colloids and Surfaces A: Physicochemical and Engineering Aspects, 366: 197-202.

Zhou, Y., Kong, Y., Kundu, S., Cirillo, J.D. and Liang, H., 2012. *Antibacterial activities of gold and silver nanoparticles against Escherichia coli and bacillus Calmette-Guerin*. Journal of Nanobiotechnology, 10: 19.

Zielińska, A., Skwarek, E., Zaleska, A., Gazda, M. and Hupka, J., 2009. *Preparation of silver nanoparticles with controlled particle size*. Procedia Chemistry, 1: 1560-1566.